

On the nature and origin of garnet in highly-refractory Archean lithospheric mantle: constraints from garnet exsolved in Kaapvaal craton orthopyroxenes

SALLY A. GIBSON

Department of Earth Sciences, University of Cambridge, Cambridge, UK CB2 3EQ

(sally@esc.cam.ac.uk)

Invited paper: 45th Hallimond Lecture

Submitted for publication in Mineralogical Magazine: July 2016.

Revised: 4th October 2016

Accepted for publication: 4th October 2016

Abstract

The widespread occurrence of pyrope garnet in Archean lithospheric mantle remains one of the 'holy grails' of mantle petrology. Most garnets found in peridotitic mantle equilibrated with incompatible-trace-element-enriched melts or fluids and are the products of metasomatism. Less common are macroscopic intergrowths of pyrope garnet formed by exsolution from orthopyroxene. Spectacular examples of these are preserved in both mantle xenoliths and large, isolated crystals (megacrysts) from the Kaapvaal craton of southern Africa, and provide direct evidence that some garnet in the sub-continental lithospheric mantle initially formed by isochemical rather than metasomatic processes. The orthopyroxene hosts are enstatites and fully equilibrated with their exsolved phases (low-Cr pyrope garnet \pm Cr-diopside). Significantly, *P-T* estimates of the post-exsolution orthopyroxenes plot along an unperturbed conductive Kaapvaal craton geotherm and reveal that they were entrained from a large continuous depth interval (85 to 175 km). They therefore represent snapshots of processes operating throughout almost the entire thickness of the sub-cratonic lithospheric mantle.

New rare-earth element (REE) analyses show that the exsolved garnets occupy the full spectrum recorded by garnets in mantle peridotites and also diamond inclusions. A key finding is that a few low-temperature exsolved garnets, derived from depths of ~90 km, are more depleted in light REEs than previously observed in any other mantle sample. Importantly, the REE patterns of these strongly LREE-depleted garnets resemble the hypothetical composition proposed for pre-metasomatic garnets that are thought to pre-date major enrichment events in the sub-continental lithospheric mantle, including those associated with diamond formation. The recalculated compositions of pre-exsolution orthopyroxenes have higher Al₂O₃ and CaO contents than their post-exsolution counterparts and most likely formed as shallow residues of large amounts of adiabatic decompression

melting in the spinel-stability field. It is inferred that exsolution of garnet from Kaapvaal orthopyroxenes may have been widespread, and perhaps accompanied cratonization at ~ 2.9 to 2.75 Ga. Such a process would considerably increase the density and stability of the continental lithosphere.

Introduction

Over the last 50 years our understanding of the thermal and compositional structure of the Earth's interior has changed dramatically. Pivotal to this transformation in scientific understanding have been findings from petrological and geochemical studies on kimberlite-borne mantle xenoliths and inclusions in diamonds; these provide the only direct information on the deep mantle, and in turn unique constraints on its long-term evolution and compositional variability (e.g. Boyd, 1989; Boyd *et al.*, 1993; Burgess and Harte, 2004; Dawson, 2004; Dawson *et al.*, 1980; Harte, 1983; Pearson *et al.*, 2014; Pearson and Wittig, 2013; Stachel *et al.*, 2004, 2005; Walter *et al.*, 2011). Information gained from pressure and temperature (P - T) estimates of these mantle fragments has been fundamental to calculation of geothermal gradients and calibration of corresponding seismic data, and key to understanding the long wave-length, spatial variability in the thermal structure and thickness of ancient continental lithosphere (e.g. (Begg *et al.*, 2009; Griffin *et al.*, 2003; Mather *et al.*, 2011; McKenzie *et al.*, 2005; Priestley and McKenzie, 2013).

Even after several decades of mantle petrology, isotope geochemistry and solid-Earth geophysics there is, however, no consensus on how the ancient cores of continents formed and information on macro-scale geodynamic processes gained from micro-scale observations and *in-situ* analyses of individual phases continues to fuel investigations on mantle peridotites. While mantle xenoliths are our only direct probes of the deep Earth, most have suffered modal and cryptic overprinting since their initial time of formation (Boyd *et al.*, 1993; Dawson, 1987), which makes deciphering their pressure-temperature and time histories complex. Much of the interpretation of the compositional evolution of the sub-cratonic mantle has focused on pyrope garnets (e.g. Burgess and Harte, 2004; Gibson *et al.*, 2008, 2013, Harte and Gurney, 1981, 1981; Ivanic *et al.*, 2016; Shu and Brey, 2015; Stachel

et al., 1998) but the widespread and variable occurrence of this high-density phase in Archean lithospheric mantle remains one of the outstanding 'holy grails' of mantle petrology. The nature and timescales of formation of garnet are important to our understanding of how the deep keels of Earth's sub-cratonic lithospheric mantle have remained stable for the last 2.5 Ga, since it potentially leads to negative buoyancy and destabilisation (Gibson *et al.*, 2013; Jordan, 1979; Lee *et al.*, 2011; Peslier *et al.*, 2010; Schutt and Lesher, 2010).

Archean sub-cratonic mantle peridotites are distinguished from those found in off-craton settings by their higher Mg# ($\text{Mg}/[\text{Mg}+\text{Fe}] \times 100$), which is commonly >92, and are considered to be more refractory melt residues (Boyd, 1989). Much of the Archean sub-cratonic lithospheric mantle is thought to consist of amalgamated residues of convecting mantle melting (Boyd *et al.*, 1993; Harte, 1983) that formed by: (i) single-stage melting in a tectonic setting analogous to present-day oceanic spreading ridges (Doucet *et al.*, 2012; Gibson *et al.*, 2008) and/or hotspots (Arndt *et al.*, 2009), but at potential temperatures up to ~ 250 °C higher (Herzberg and Rudnick, 2012; Lee and Chin, 2014; Richter, 1988); or (ii) multi-stage shallow melting, initially beneath a spreading ridge followed by hydrous remelting in a convergent tectonic setting (Carlson *et al.*, 2005; Pearson and Wittig, 2008; Shu *et al.*, 2013; Simon *et al.*, 2007). Despite these different opinions on the melting regime, Re-Os model ages indicate that melt depletion events associated with the initial formation of sub-cratonic lithospheric mantle were ancient and occurred between 3.5 and 2.5 Ga (Pearson *et al.*, 1995; Walker *et al.*, 1989). The paradox is that garnet often occurs in mantle lithologies depleted in clinopyroxene (dunites and harzburgites), which represent residues of major melting events involving up to 40% partial melting, whereas experimental studies on fertile peridotite suggest that garnet should be exhausted by <20 % melting (Figure 1; Herzberg, 2004; Simon *et al.*, 2003; Walter, 1998).

The compositions of pyrope garnets commonly found in mantle peridotite suites are diverse and generally vary in accordance with paragenesis (Burgess and Harte, 2004; Grütter *et al.*, 2004; Gurney *et al.*, 1979; Gurney and Switzer, 1973; Sobolev *et al.*, 1973). For example, garnets from harzburgites have low CaO contents and are often 'sub-calcic' whereas those found in lherzolites have higher CaO contents, and show a steep positive correlation with Cr₂O₃ (Figure 2). Typically, pyrope garnets from lherzolitic sub-cratonic mantle are enriched in strongly-incompatible trace elements from which equilibrium with high-pressure, small-fraction, volatile-rich, metasomatic mantle melts or fluids has been deduced (e.g. Gibson *et al.*, 2013; Shu and Brey, 2015; Stachel and Harris, 1997). A substantial overlap exists between sub-calcic garnets found in harzburgites and those in diamond inclusions (Stachel and Harris, 2008) and suggests that they represent garnets from the early formation of the sub-continental lithosphere. The discovery of: (i) rare garnets with ultra-depleted CaO (<2 wt. %; Figure 2) and/or very-low incompatible-trace-element contents (Dawson, 2004; Gibson *et al.*, 2013); and (ii) exsolution lamellae of garnet in orthopyroxene (Aoki *et al.*, 1980; Dawson, 2004; Dawson *et al.*, 1980; Egglar *et al.*, 1979) suggest that at least some pyrope garnets in the lithospheric mantle have an isochemical rather than a metasomatic origin.

The scarcity of garnets with exceptionally-low CaO is almost certainly because less than 1 % of the mantle sampled by xenoliths and megacrysts is unmetasomatised (Pearson and Wittig, 2013) and the extent to which sub-cratonic lithospheric mantle has been affected by exsolution of garnet from orthopyroxene (enstatite) remains enigmatic; much more widely reported is the exsolution of garnet from clinopyroxene in mantle eclogites and pyroxenites rather than peridotites (Beeson and Jackson, 1970; Faryad *et al.*, 2009; Harte and Gurney, 1975; Jerde *et al.*, 1993; Roach, 2004; Sautter and Harte, 1988, 1990; Wilkinson, 1976). Here, I present detailed descriptions of mineral microstructures together

with the first *in-situ* major- and trace-element analyses of pyrope garnets found as exsolution lamellae in enstatites. Geo-thermobarometry shows that sub-solidus exsolution occurs over an extensive depth range in the Kaapvaal lithospheric mantle. This supports the hypothesis that isochemical formation of garnet is not a localised feature and hence of importance to our understanding of the evolution and long-term stability of the lithospheric mantle.

Evidence for isochemical formation of pyrope garnet in the lithospheric mantle

Low Ca and Cr (“ultra-depleted”) pyrope garnets

Published reports of pyrope garnets formed by isochemical exsolution are abundant in the literature. A small number of pyrope garnets with ultra-depleted major- and/or trace-element compositions have been found in mantle peridotites from the Tanzanian and Kaapvaal cratons (Gibson *et al.*, 2013; Lazarov *et al.*, 2009, 2012; Shu and Brey, 2015), and also in xenocryst suites from the Siberian, North Atlantic and Superior cratons (Grütter and Tuer, 2009; Ziberna *et al.*, 2013). They are distinguished by their very low CaO contents (<2 wt. %; Grütter *et al.*, 2004). Ultra-depleted garnets found in mantle peridotites from the Tanzanian sub-cratonic mantle (at Lashaine) are especially notable because they have very low concentrations of light rare-earth-elements (LREEs) that are similar to those of hypothetical garnets thought to have formed prior to metasomatism of the Earth’s sub-cratonic mantle (Gibson *et al.*, 2013). These rare Ca- and Cr-poor garnets coexist in chemical and textural equilibrium with highly-refractory olivine (Fo_{95.4}) and orthopyroxene (Mg#=96.4). Importantly, all of these phases are more magnesian than generally encountered in global samples of depleted lithospheric mantle, *i.e.* harzburgites and

diamond inclusion suites (Gibson *et al.*, 2013). The Tanzanian ultra-depleted garnets form interconnecting networks ('necklaces') around grains of orthopyroxene, which together with the major, trace and REE contents of the garnets implies an origin by isochemical exsolution involving diffusion of large cations (Si^{4+} and Al^{3+}) to grain boundaries during sub-solidus cooling. The ultra-depleted Tanzanian garnets occur in low-temperature (~ 1050 °C) peridotite xenoliths derived from depths of ~ 120 km, *i.e.* shallower than those normally reached by percolating metasomatic melts and fluids in this region, and have not been metasomatised by their transporting melts (Gibson *et al.*, 2013).

Occurrences of garnets with ultra-low CaO contents may be rare because: (i) their low CaO concentrations make them readily susceptible to geochemical overprinting by Ca-rich metasomatic melts (e.g. Burgess and Harte, 2004; Gibson *et al.*, 2013; Griffin *et al.*, 1999a; Schulze, 1995) and (ii) highly-refractory peridotite is more common in the 'shallow' lithospheric mantle but is not normally brought to the surface by ascending melts, which tend to metasomatise and preferentially sample their source regions in the deeper mantle. Nevertheless, the depleted compositions of these garnets offer important evidence that they are not solely a result of fractional crystallisation and/or reaction of percolating, incompatible-trace-element-rich, metasomatic agents in the sub-cratonic lithospheric mantle (Eggler and Wendlandt, 1982; Gurney *et al.*, 1979).

Garnet exsolution from orthopyroxene in megacrysts and peridotite xenoliths from the Kaapvaal sub-cratonic lithosphere

Olivine, orthopyroxene, clinopyroxene, garnet, ilmenite and phlogopite often occur as large (>2 cm), single "megacrysts" in kimberlites (Dawson, 1980). Suites of these mantle megacrysts vary in terms of their compositions and have been divided into: (i) a Cr-poor megacryst suite, which contains garnet, orthopyroxene, clinopyroxene and ilmenite with

low Cr₂O₃, high TiO₂ contents and variable Mg# (Harte and Gurney, 1981); and (ii) a less-common, Cr-rich megacryst suite with compositions similar to those found in mantle peridotites (Eggler *et al.*, 1979; Moore and Costin, 2016). A further suite of orthopyroxene megacrysts, distinguished by their coarse exsolution lamellae (c.f. fine exsolution lamellae present in Cr-poor and Cr-rich orthopyroxene megacrysts) has also been described (Eggler *et al.*, 1979). These orthopyroxene megacrysts are characterised by much lower CaO at a given Al₂O₃ content and extend to more Mg-rich compositions than orthopyroxenes in the Cr-poor and Cr-rich megacryst suites (Gurney *et al.*, 1979).

Cr-poor megacrysts crystallise over a wide range of temperatures (1050 to 1400 °C) in the lower sub-cratonic lithosphere and have been linked via their large size, compositions and ages to fractional crystallisation of percolating, metasomatic, kimberlite-like melts (Harte *et al.*, 1993). The sub-microscopic exsolution lamellae in both the Cr-poor and -rich orthopyroxene megacrysts most likely formed by relatively rapid cooling whereas the orthopyroxenes containing macroscopic exsolved garnet are thought to have cooled slowly and represent fragments of ancient lithospheric mantle (Harte and Gurney, 1981). Both fine and coarse garnet exsolution lamellae have been described in orthopyroxene found as megacrysts at Frank Smith and Bellsbank diamond mines in the classic Kimberley area and in a lherzolite xenolith (BD1366) from Monastery Mine, Lesotho (Aoki *et al.*, 1980; Dawson, 2004; Dawson *et al.*, 1980). In the latter, garnet occurs (i) together with Cr-spinel and Cr-diopside as fine-scale exsolution lamellae in a large porphyroclast of orthopyroxene (enstatite), and (ii) as a 'necklace' along orthopyroxene grain boundaries (Dawson, 2004). These exsolution textures are closely associated with deformation textures (kink banding) in the enstatite host and appear to be linked to strain of the crystal lattice (Dawson, 1981).

Analytical Methods

In this study, modal proportions of mineral phases were determined by tracing grain boundaries in digital scans and then calculating the areas occupied by each phase using the open-source, image-processing package Fiji[®]. Orthopyroxene, clinopyroxene and garnet were analysed in 13 samples for major and some trace elements using a Cameca SX100 electron microprobe in the Department of Earth Sciences at the University of Cambridge (Table 2). This was equipped with five wavelength-dispersive spectrometers and one energy-dispersive spectrometer. Trace-element concentrations in garnet were determined in 5 of these samples using a New Wave UP213 Nd:YAG laser ablation system interfaced to a Perkin-Elmer Elan DRC II ICP-MS in the Department of Earth Sciences at the University of Cambridge (Table 3). An 80 µm diameter beam and a laser repetition rate of 10 Hz at a power of ~1 mJ (10 J cm⁻²) were used for the entire study. The spot size was chosen as a compromise between signal intensity and the size of the minerals of interest in the samples. Further details of analytical techniques are provided in Supplementary Files.

Petrographic description of orthopyroxene and exsolved garnet

This investigation is based on 3 mantle peridotites and 26 orthopyroxene megacrysts collected in the 1960's by JB Dawson from various kimberlite localities (mines) in central and southern parts of the Kaapvaal craton (Frank Smith, Bultfontein and Wesselton in the Kimberley area, Jagersfontein and Monastery). The orthopyroxene megacrysts occur as euhedral, stout prisms up to several centimeters in length. They are fresh and many contain visible crystals of pink-purple garnet and, to a lesser extent, emerald-green clinopyroxene (Figure 3). Microstructures in the orthopyroxenes -- such as undulose extinction and

oriented, fine lamellae -- are most evident in cross-polarised light (Figure 4). The textures associated with the exsolved garnet can be subdivided into four types:

- (i) *Fine closely-spaced lamellae or rods.*
- (ii) *Isolated blebs of exsolved garnet in single grains of orthopyroxene.* This texture is the least common. The blebs are elongate and sometimes have spindle shapes with a preferred orientation, parallel to {110} of the host orthopyroxene (e.g. BD1959, Wesselton Mine, Figure 4a).
- (iii) *Veinlets or chains of rounded grains of pale-pink garnets within orthopyroxene grains.* Their orientation varies from parallel, to inclined and/or perpendicular to the cleavage (e.g. BD2015/3a, Frank Smith Mine, Figure 4b).
- (iv) *Necklace texture* formed of equant grains of pale-pink garnet. The interconnected networks of stringers extend over several centimetres along orthopyroxene grain boundaries (e.g. BD1951, Bultfontein Mine, Figure 4c). Clinopyroxene also sometimes occurs along grain boundaries in close association with the garnet.

In orthopyroxene megacrysts, garnet tends to be the dominant exsolved phase and may occupy up to ~25% of the crystal (Table 1). The highest proportion of orthopyroxene occurs in megacrysts that contain isolated blebs of garnet (Figure 4a). Intra-grain exsolution of garnet is best preserved in large orthopyroxene grains (*i.e.* megacrysts). This is presumably because in the smaller grains (< 10 mm), which are often found in peridotite xenoliths, diffusion lengths of Al³⁺ and Si⁴⁺ are such that garnet nucleates in interconnected networks of crystals on orthopyroxene grain boundaries. Clinopyroxene only occurs in small modal amounts (<6%) and forms rods or blebs with deformation twins (Figure 4a). Minor secondary phlogopite was observed in a few samples (Table 1).

Multi-stage, multi-phase exsolution in a single orthopyroxene megacryst

The wide variety of exsolution styles are strikingly displayed in a single enstatite megacryst BD3736/1 (Figure 7). These offer a unique insight into the sub-solidus cooling history of sub-cratonic lithosphere and hence are described in detail below.

Megacryst BD3736/1 was entrained by the 86 Ma Jagersfontein kimberlite (Smith *et al.*, 1985). The host enstatite, which is 20 mm long and 10 mm wide and shows undulatory extinction, contains 23% exsolved garnet and 2% exsolved clinopyroxene (Table 1). The exsolved garnets occur as elongate, 1.5 mm wide grains that form evenly-spaced (4 mm) chains parallel to {001} of the orthopyroxene host. Coarse, 'spindle-shaped' blebs and also fine lamellae of clinopyroxene occur perpendicular to the exsolved garnet chains, and are parallel to {110} of the host orthopyroxene (Figure 7 & 8). The clinopyroxene blebs occur at evenly spaced intervals (0.75 mm) along orthopyroxene-garnet grain boundaries and often extend out into the host orthopyroxene forming thin 'tails' (Figure 8 & Supplementary Figure). These coarse exsolved clinopyroxenes sometimes cut across the garnet chains. The fine clinopyroxene lamellae are 3.5 μm in length and occur at intervals of $\sim <10 \mu\text{m}$. They are best developed away from the chains of exsolved garnet so that $\sim 0.3 \text{ mm}$ wide, lamellae-free zones (haloes) occur in the orthopyroxene adjacent to the garnets. Also, at the junction of the garnets and orthopyroxenes there are low-angle, planar, sub-grain boundaries that show evidence of dislocation climb. These are variably offset around different garnet grains. Where they occur in dislocation zones, the fine clinopyroxene lamellae show evidence of refraction, usually near their terminations.

Variations in mineral chemistry of host orthopyroxene, exsolved garnet and clinopyroxene

The major-element analyses show that all of the studied orthopyroxene megacrysts are enstatites (Mg#=63-94) with low CaO and Al₂O₃ contents and, most importantly, are

typical of those found in garnet-bearing mantle peridotites (Figure 5). At Monastery, Jagersfontein, Bultfontein and Wesselton the orthopyroxenes have high Mg# (89 to 94) and Cr₂O₃ (0.21 to 0.4 wt. %), and low but variable contents of both CaO (0.2 to 0.45 wt. %) and Al₂O₃ (0.7 to 0.9 wt. %; Table 2). In BD3736/1 the orthopyroxene host is a high Mg# (93.3), CaO (0.2 wt. %) and Al₂O₃-rich (0.9 wt. %) enstatite (Table 2). A subtle increase (from 0.7 to 0.9 wt. %) in Al₂O₃ was observed in the halo adjacent to the exsolved garnet. Orthopyroxenes from Frank Smith Mine are distinctive because of their wide ranges of Mg# (84 to 93), CaO (0.2 to 0.59 wt. %) and Al₂O₃ contents (0.55 to 0.88 wt. %; Table 2).

The exsolved garnets are pyropes with a wide range in Mg# (63 to 87). While garnets in individual samples are compositionally uniform those from different samples have highly variable Cr₂O₃ (1.8 to 5.6 wt. %) but restricted CaO contents (4.4 to 5.7 wt. %) and in these respects resemble mantle garnets of lherzolite paragenesis (Figure 2). The exsolved garnets in BD3736/1 have a uniform composition and are characterised by high Mg# (82) and TiO₂ (0.02 wt. %). Their CaO (4.6 wt. %) and Cr₂O₃ (1.86 wt. %) contents are among the lowest observed in the Kaapvaal orthopyroxene megacryst suite (Table 2 & Figure 2). Garnets from Frank Smith Mine extend to higher CaO at a given Cr₂O₃ content. All of the exsolved garnets have low TiO₂ contents (<0.1 wt. %) and are similar to discrete garnet grains found in lherzolites.

The exsolved clinopyroxenes are characterised by high Ca/(Ca+Mg) ratios (0.45 to 0.50), Mg# (87 to 95) and Cr₂O₃ contents (1.4 to 2.9 wt. %) and are therefore Cr-diopsides (Stephens and Dawson, 1977). The Mg# of the clinopyroxene is usually similar to the orthopyroxene host but Cr₂O₃ contents are much higher. In BD3736/1 the clinopyroxene blebs are more magnesian (Mg#=95) than the fine clinopyroxene exsolution lamellae (Mg#=91). The lowest Mg# and Cr₂O₃ contents are found in clinopyroxenes exsolved in orthopyroxene megacrysts from Frank Smith Mine. Like the garnets, the clinopyroxenes are

characterised by low TiO_2 (<0.2 wt. %), but have moderate Na_2O (1.4 to 2.6 wt. %) and Al_2O_3 contents (1.4 to 2.9 wt. %), and resemble those found in lherzolites.

Given the large variations in major-element contents of the exsolved garnets it is unsurprising that they also show a large range in trace element concentrations. The highest concentrations of incompatible trace elements (Hf, Sr, Ti, Y and Zr) were found in garnets exsolved from orthopyroxene megacryst BD1959 (Wesselton; [Table 3](#)) and in a necklace around an orthopyroxene in peridotite BD3635 (Kimberley). On a chondrite-normalised REE plot ([Figure 6](#)), these garnets display a 'normal' pattern, *i.e.* they have low concentrations of light REEs (0.5 to 11 x chondrite) and similar, moderate concentrations of middle to heavy REEs (12-20 x chondrite). Garnets from 2015/5 (Frank Smith Mine) display mildly-sinusoidal REE patterns and have concentrations of light and heavy REEs that are much lower than those in BD1959. The different REE patterns are not restricted to individual localities, however. At Wesselton exsolved garnets with 'normal' patterns occur together with those that have strongly-sinusoidal chondrite-normalised REE patterns (e.g. BD1942). The latter exhibit a maxima at Sm and a minima at Er ([Figure 6](#)). They have low but variable La and Ce concentrations, and the lowest concentrations of heavy REEs out of all of the exsolved garnets analysed. Exsolved garnets in orthopyroxene megacryst BD3736/1 (Jagersfontein) are especially notable because they have extremely-low concentrations of Hf, Nb, Pb, Rb, Th, U, Zr and LREEs, which are often below detection limits ([Table 3](#)). Concentrations of light REEs are < 0.04 x chondrite and heavy REEs are up to 10 x chondrite. As a consequence, garnets from BD3736/1 have very steep slopes on normalised REE plots ([Figure 6](#)).

Reconstructed primary orthopyroxene compositions

The reconstructed bulk compositions of pre-exsolution Kaapvaal orthopyroxene megacrysts are shown in [Table 4](#). These are calculated from the major-element chemistry

and modal proportions of both the exsolved and host phases (Tables 1 & 2). The pre-exsolution megacryst compositions all have the correct stoichiometry for orthopyroxene but they are highly variable in terms of Mg# (84 to 93.5), Al₂O₃ (0.8 to 5.8 wt. %) and CaO contents (0.8 to 5.6 wt. %). It is noteworthy that the Mg# of both the reconstructed pre-exsolution orthopyroxene (Table 4) and post-exsolution orthopyroxene megacrysts (Table 1) are similar and do not appear to have changed during exsolution. This is consistent with the findings of von Seckendorff and O'Neill (1993) which showed that the Fe/Mg in orthopyroxene is controlled by bulk-rock composition and relatively insensitive to changes in temperature and pressure. In contrast to Mg#, contents of both CaO and Al₂O₃ are noticeably greater (Figure 5) and the SiO₂ content lower in the pre-exsolution orthopyroxene.

Final *P-T* estimates for Kaapvaal orthopyroxene megacrysts and mantle peridotites

The presence of co-existing orthopyroxene, garnet and sometimes clinopyroxene allows final equilibration pressures and temperatures (*i.e.* post exsolution) of the Kaapvaal megacrysts and peridotite xenoliths to be estimated. Combinations of the two-pyroxene solvus thermometer of Taylor (1998), the Ca-in-orthopyroxene thermometer of Brey & Köhler (1990) and the garnet-orthopyroxene Al-barometer of Nickel & Green (1985) were used iteratively to estimate temperatures and pressures, as recommended by Nimis & Grütter (2009). These geo-thermometers and -barometers rely on major-element contents of various co-existing minerals and assume that the phases are fully equilibrated. The extent of equilibrium in co-existing mineral phases was established following the recommendations of Nimis & Grütter (2009). An initial check was made by comparing temperatures estimated for samples bearing both clinopyroxene and orthopyroxene. These showed only a slight

difference (less than 30°C) for the two-pyroxene solvus (Taylor, 1998) and Ca-in-orthopyroxene thermometers (Brey and Kohler, 1990; Figure 9). Some of the samples from Jagersfontein, Frank Smith and Monastery equilibrated at temperatures outside the lower bound of experiments used by Taylor (1998), i.e. <900 °C. Brey & Kohler (1990) showed that at these low temperatures the Ca-in orthopyroxene parameterisation gives slightly high values but the excellent positive correlation between the results from the two thermometers ($R^2=0.968$) confirms that the orthopyroxene and exsolved clinopyroxene are fully equilibrated. The temperatures obtained for both clinopyroxene-bearing and clinopyroxene-free samples are therefore internally consistent regardless of the parameterisation used.

Pressure estimates for Kaapvaal samples containing fully-equilibrated orthopyroxene and exsolved garnet range from 26 to 53 kbars, which correspond to a depth interval of 85 to 175 km in the lithosphere. Temperature estimates for the same samples are also highly variable, ranging from 700 to 1100 °C (Table 2 & Figure 10). Importantly, Figure 10 shows that co-variations in temperature and pressure recorded by these samples correspond almost exactly to the 45.6 mW/m² conductive geotherm for kimberlite-hosted mantle peridotites from Finsch Mine in the western Kaapvaal craton (Gibson *et al.*, 2008; Lazarov *et al.*, 2009). Xenoliths from the 118 Ma Finsch kimberlite (Smith *et al.*, 1985) were entrained over a large depth interval and define a geotherm that is less perturbed at the base of the lithosphere than those hosted by some more recent Kaapvaal kimberlites, which are thought to be affected by regional heating events (Bell *et al.*, 2003). *P-T* estimates from Finsch suggest that the base of the mechanical boundary layer beneath the Kaapvaal craton is at a depth of ~204 km (Figure 10). The deepest orthopyroxenes exhibiting exsolution of garnet that were examined in this study were therefore entrained from within 30 km of this major boundary.

Discussion

The orthopyroxenes with exsolved garnet that were examined in this study are remarkably fresh and offer a new perspective on the garnet paradox. The lack of any signs of dissolution of the megacrysts is somewhat surprising, given the susceptibility of orthopyroxenes to react with silica-undersaturated melts during transport to the surface (Bussweiler *et al.*, 2016; Russell *et al.*, 2012; Soltys *et al.*, 2016), and the extent to which the orthopyroxenes have interacted with the host kimberlite is limited. While thin veins that cross-cut the exsolved garnets in the orthopyroxene megacrysts may be evidence of post-entrainment interaction and kimberlite infiltration, the variability in enrichment of the LREEs in the exsolved garnets appears to be depth dependent, i.e. occurred prior to entrainment, such as at Wesselton where a variety of different styles of REE enrichment is evident (Figure 6).

What are the crystal controls on garnet exsolution from orthopyroxene?

The results of the high temperature (1450 to 1525 °C) and pressure (<4.5 to 5.5 GPa) experiments of Canil (1991) suggest that both garnet and clinopyroxene might form in the lithospheric mantle as a result of sub-solidus isochemical exsolution from orthopyroxene. It is anticipated that the size and spacing of the exsolved garnets will vary systematically according to diffusion mechanisms and decrease with the rate of sub-solidus cooling. Greater insights into this process are provided by enstatite-rich megacryst BD3736/1, which records the variable length scales of diffusion that accompanies sub-solidus cooling and exsolution (see above). The multi-stage exsolution involved in the cooling of this megacryst is interpreted as follows:

- (i) At high sub-solidus temperatures enstatite with high contents of CaO and Al₂O₃ behaves as a monoclinic crystal (clino-enstatite) and exsolves pyrope garnet parallel to {001}. Equant 2-3 mm grains of garnet coalesce into widely-spaced chains.
- (ii) Sub-solidus exsolution and diffusion of large cations (Ca²⁺, Al³⁺ and Si⁴⁺) causes clino-enstatite to invert to ortho-enstatite, perhaps promoting deformation of the crystal lattice.
- (iii) This exsolution of clinopyroxene (Mg#=95), and nucleation occurs as equally-spaced 'spindle-shaped' blebs along orthopyroxene-garnet grain boundaries and parallel to {110} (Figure 8).
- (iv) This nucleation and growth of coarse garnet and clinopyroxene creates depletion 'haloes' in the host orthopyroxene (Figure 8).
- (v) Homogeneous nucleation and crystallisation of clinopyroxene takes place away from the depletion 'haloes' associated with previously exsolved garnet and clinopyroxene, to form equally-spaced fine lamellae (Mg#=91) parallel to {110}.
- (vi) Finally, dislocation creep results in planar, sub-grain boundaries parallel to garnet-orthopyroxene grain boundaries.

Isochemical exsolution of garnet from orthopyroxene during lithospheric cooling

A key finding from the thermobarometry is that garnet is exsolving from orthopyroxene throughout most of the depth range where garnet is stable (85-175 km) in the Kaapvaal lithospheric mantle, which implies that this is not a localised process. In this study, evidence that some of the exsolved garnets have interacted with percolating metasomatic fluids and melts is provided by their rare-earth-element patterns. It can be seen from Figure 6 that the 'normal' and 'sinusoidal' REE patterns displayed by the exsolved garnets resemble those exhibited by global garnets of Iherzolitic and harzburgitic paragenesis, respectively. A

significant observation from this study is that garnet and clinopyroxene with the most highly-depleted in strongly-incompatible trace element concentrations were exsolved from orthopyroxene megacrysts which were entrained from the shallowest depths (~90 km) and lowest temperatures (~700 °C; Figure 6). While this is most profound for Jagersfontein megacryst BD3736/1, garnets with low Cr₂O₃ (<3 wt. %) and REE abundances are also found exsolved in fully-equilibrated orthopyroxene megacrysts that were entrained from shallow depths in the lithospheric mantle beneath Wesselton and Frank Smith Mines.

The low concentrations of trace elements that characterise some of the exsolved garnets (*e.g.* BD3736/1, Table 3) are highly significant because they are similar to the hypothetical composition proposed for mantle garnets prior to metasomatism by fluids and small-fraction kimberlite-like melts (Shu and Brey, 2015; Stachel *et al.*, 2004; Ziberna *et al.*, 2013; Figure 11a). The heavy REE contents of the hypothetical compositions were estimated from the Dy to Lu slope on chondrite-normalised REE plots of sub-calcic garnets whereas the light and middle REEs (La to Tb) were calculated from experimental melt partition coefficients (*e.g.*, Johnson, 1998). A further important finding is that the most LREE-depleted exsolved garnets have even lower concentrations of La, Ce, Pr and Nd than the most LREE-depleted garnets found to date in both peridotite xenoliths (from Tanzania; Gibson *et al.*, 2013) and diamond inclusion suites, *e.g.* from Kankan and Yakutia (Stachel *et al.*, 2000; Taylor *et al.*, 2003); Figure 11b, c, d). The latter is significant because once having been encapsulated by diamonds, garnets are protected from later metasomatic events (Shu and Brey, 2015) and their REE patterns reveal enrichment that may pre-date or coincide with diamond formation (Figure 11e).

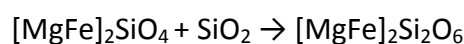
The 'normal' REE patterns of lherzolitic garnets resemble those generated in experiments on primitive mantle melts (*e.g.* Tuff & Gibson, 2006; Figure 11f) and are commonly associated with melt-related mantle metasomatism, whereas the sinusoidal REE

patterns are similar to those of harzburgitic garnets that are thought to result from the infiltration of low-temperature fluids (Stachel *et al.*, 1998; Stachel and Harris, 1997) or carbonatitic melts (Shu and Brey, 2015). An interesting paradox arises from the fact that while all of the exsolved garnets have a lherzolitic affinity in terms of their CaO and Cr₂O₃ contents (Figure 2) some of their REE patterns resemble those found in mantle harzburgites (Figure 11f). This dichotomy most likely arises because the REEs are incorporated in garnet via exchange with divalent cations that occupy the eight-fold site other than simply Ca (e.g. Mg; Orman *et al.*, 2002). Also, garnet has high partition coefficients for many incompatible trace elements, relative to olivine and orthopyroxene, and numerical models show that only a small percentage of fluid or melt is required to change the REE pattern from strongly LREE-depleted to 'normal' (Gibson *et al.*, 2013; Shu and Brey, 2015).

Beneath southern Africa, craton-scale metasomatism has been multi-phase (Kramers *et al.*, 1983; Menzies & Murphy, 1980; Shu *et al.*, 2013) and is most prevalent in the lower part (130-200 km) of the Kaapvaal lithosphere, where it is associated with deformed high-temperature peridotites. At shallow depths (<105 km) -- and where orthopyroxene megacryst BD3736/1 was entrained -- the lithospheric mantle is characterised by coarse, low-temperature peridotites that bear garnets which have largely escaped metasomatism (Burgess and Harte, 1999, 2004). Since only a very small proportion (approximately 5%) of the Kaapvaal lithospheric mantle is formed of harzburgite (Schulze, 1995), and hence has remained immune from chemical over-printing, it is not surprising that incompatible-trace-element-depleted signatures such as those observed in exsolved garnets from BD3736/1 are rare.

In comparison to many of the world's other cratons the lithospheric mantle underlying the eastern and central parts of the Kaapvaal, Tanzanian and northern Siberian

cratons is unusually rich in orthopyroxene (Boyd, 1989; Boyd and Mertzman, 1987; Griffin *et al.*, 1999b; Rudnick *et al.*, 1994). Of these, the lithospheric mantle beneath the Kaapvaal craton contains the greatest amount of orthopyroxene and is present in almost two-fold the abundance of average Archean cratonic mantle (Table 5). This “excess” in orthopyroxene (enstatite) occurs at the expense of olivine and requires that bulk-rock Mg# remains constant but SiO₂ contents are increased. The formation of excess orthopyroxene appears to have taken place prior to or during lithospheric thickening, thermal consolidation and stabilisation (*i.e.* cratonisation) at ~2.9 to 2.75 Ga and has variously been attributed to: (i) extraction of komatiite melts in the Archean (Boyd, 1989; Doucet *et al.*, 2012); (ii) crystallisation from an SiO₂-rich ultrabasic magma (Herzberg, 1993: 1); (iii) phase transformation from olivine to orthopyroxene by reaction with percolating silicic fluids, rich in Al, Ca and Na (Kelemen *et al.*, 1998; Kesson and Ringwood, 1989; Rudnick *et al.*, 1994).



The high Mg# of many of the pre-cursor orthopyroxenes is consistent with their formation as either a residue of mantle melting or a reaction product of a silicic fluid with Fo-rich olivine, rather than crystal fractionation from a more Fe-rich kimberlite host.

Control of orthopyroxene composition and sub-solidus cooling on garnet exsolution

In the Kaapvaal orthopyroxenes studied here there is no correlation between either the style of garnet exsolution or presence/absence of Cr-diopside with temperature or pressure. This suggests that their formation is dependent upon the composition of the host orthopyroxene and consistent with the findings of Canil (1991), which showed that the ability of orthopyroxene (enstatite) to exsolve pyrope garnet and/or Cr-diopside during sub-solidus cooling of the mantle is dependent upon Al₂O₃ and CaO contents. Concentrations of

these oxides vary systematically in orthopyroxenes that formed as melt residues in different tectonic settings (see Gibson *et al.*, 2008 and [Figure 5](#)): those in garnet harzburgites from on-craton settings usually have a restricted range of Al_2O_3 (< 1 wt. %) and CaO (0.5 wt. %) whereas orthopyroxenes in spinel harzburgites from off-craton and oceanic settings exhibit a much wider positive correlation between Al_2O_3 (up to 6 wt. %) and CaO (up to 2 wt. %). [Figure 5](#) shows that most of the recalculated, bulk pre-exsolution compositions of Kaapvaal orthopyroxenes are characterised by high Al_2O_3 relative to typical cratonic orthopyroxene and plot in the field of spinel-bearing off-craton or abyssal peridotites. Exceptions are the recalculated, pre-exsolution compositions of orthopyroxene megacrysts from Frank Smith Mine which have very high CaO but low Al_2O_3 contents; in this respect they are similar to orthopyroxenes found in metasomatised and sheared, high-temperature garnet peridotites (Iherzolites, [Figure 5](#)).

The high Mg# (91-94) estimated for the pre-exsolution orthopyroxenes (except those from Frank Smith Mine) are characteristic of those found in depleted harzburgites, which are thought to have formed as residues of a large amount of upwelling and adiabatic decompression melting (Boyd *et al.*, 1993; Harte, 1983; O'Hara *et al.*, 1975). If reaction of olivine with silicic fluids was also involved in the formation of the orthopyroxene this would require highly-forsteritic olivine to transform to high-Mg# orthopyroxene. While the orthopyroxenes show no geochemical evidence for this process it might offer a plausible explanation for the large size of the orthopyroxene crystals. Regardless of this uncertainty, the large amounts of decompression melting required to explain the high Mg# of the pre-exsolution orthopyroxenes (Herzberg, 2004) imply that they are associated with residues that formed as a consequence of large amounts of melting at relatively low pressures (< 2.5 GPa) in the melting regime, i.e. at significantly lower pressures than those at which the orthopyroxenes exhibiting garnet exsolution equilibrated in the lithospheric mantle prior to

their entrainment (Table 4). Although at shallow pressures the stable Al-bearing mantle phase would be spinel (Figure 12) it is unlikely that this would exist in the residue at such high degrees of melting.

The dominant control on diffusion and sub-solidus exsolution is temperature. While there remains a lack of consensus as to the processes involved in cratonization (e.g. Arndt *et al.*, 2009; Aulbach, 2012; Pearson and Wittig, 2008) it seems plausible that the coarse exsolution textures in the orthopyroxenes correspond to slow cooling, from near-anhydrous peridotite solidus conditions in the Archean to those of the present-day sub-cratonic conductive geotherm. The final recorded equilibration temperatures of the orthopyroxenes are well below that of their formation (Table 4), as either a melt residue or reaction product of olivine with silicic fluids prior to cratonization (i.e. > 2.5 Ga). Beneath the cratons the gradient of the conductive geotherm (i.e. dP/dT) is smaller than that of the anhydrous peridotite solidus so that the subsolidus cooling interval (ΔT) varies with pressure (Figure 10).

$$\Delta T(^{\circ}\text{C}) = T_{\text{anhydrous solidus}} - T_{\text{conductive geotherm}}$$

Based on a conductive geotherm of 45.6 mW/m² for the Kaapvaal craton, ΔT corresponds to ~ 700 °C at a pressure of 2.5 GPa and decreases to 500 °C at 4.5 GPa (Figure 10). The experiments of Canil (1991) indicate that, under these circumstances, garnet would start to exsolve from orthopyroxene at ~200 °C below the solidus. Diffusion of Ca²⁺, Al³⁺ and Si⁴⁺ from the orthopyroxene lattice below this temperature would continue to the final cooling temperature defined by the conductive geotherm, i.e. over a temperature interval of < 500 °C. The ΔT calculations shown in Table 4 assume that the exsolution process is isobaric, which is a simplified approach since garnet would almost certainly be exsolving over a range of pressures. Even with this assumption it is not straight forward to calculate

the amount of time for garnet to form thick lamellae in mantle orthopyroxenes. This is because: (i) the diffusion rate of Al in orthopyroxene is poorly constrained (Chin *et al.*, 2015) and (ii) the cooling rate of cratonic lithosphere -- since its time of isolation from the convecting mantle and subsequent stabilisation >2.5 Ga -- is poorly known. Estimates from isotopic studies of mantle xenoliths and geophysical investigations for cooling of the cratonic lithosphere range from 0.04 to 0.1 °C/Ma (Bedini *et al.*, 2004; Michaut and Jaupart, 2007; Shu *et al.*, 2014). Such a slow cooling rate would readily explain the sub-solidus exsolution of garnet from orthopyroxene during the last 2.5 Ga, over the 500 to 700 °C interval between the dry peridotite solidus. Nevertheless, the occurrence of garnet lamellae in mantle orthopyroxene from much younger terranes indicates that this process may be much faster (see below).

Is the Sierra Nevada continental arc (western USA) a Mesozoic analogue for garnet exsolution in thickened Archean lithosphere?

The mechanisms that occurred during the exsolution of garnet in orthopyroxenes from the Kaapvaal craton are unclear but may be similar to those recently inferred from peridotite xenoliths from the Late Mesozoic Sierra Nevada continental arc in California (Chin *et al.*, 2012, 2015). The Sierra Nevada garnets occur as rods and lamellae in orthopyroxene as well as discrete grains and coronas around spinel. The width of the exsolved rods and lamellae ranges from 100 nm to 30 µm, and therefore at a much-finer length scale than observed in the Kaapvaal orthopyroxenes described above. Both the exsolved and discrete Sierra Nevada garnets have similar CaO (4 to 5.5 wt. %) but slightly lower Cr₂O₃ contents (1 to 2 wt. %) than the exsolved Kaapvaal garnets, and are also “lherzolitic” (Figure 2). The Sierra Nevada garnets are, however, less magnesian (Mg#=75-80) than the exsolved

Kaapvaal garnets (Mg#=63-87) and have elevated concentrations of REEs (HREEs are up to ~ 50 x chondrite, [Figure 11b](#)). The most LREE depleted analyses of Sierra Nevada garnets are from the cores of discrete grains and exsolved lamellae, and their overall REE patterns resemble the strongly-LREE depleted garnets exsolved in Kaapvaal orthopyroxene megacryst BD3736/1 ([Figure 11a](#)). In contrast to the Kaapvaal samples, some Sierra Nevada garnets are not fully equilibrated and their rims exhibit mildly-sinusoidal patterns that are similar to some Kaapvaal megacrysts (e.g. BD2015/5, [Table 3](#)).

The lower temperatures of the convecting mantle in the Mesozoic compared to the Archean would decrease the depth and amount of partial melting of upwelling peridotite may well explain the generally lower Mg# of Sierra Nevada host orthopyroxenes (mean Mg#=91.5) and their exsolved garnets. The higher Mg# of the Kaapvaal orthopyroxenes (mean Mg#=92.6, excl. Frank Smith Mine) may account for their lower REE concentrations since the REEs are thought to partially substitute for Mg in garnet (Orman *et al.*, 2002). The sinusoidal REE patterns displayed by the rims of some of the Sierran garnets and also garnet coronas around spinel may be linked to a refertilisation event immediately prior to entrainment (Chin *et al.*, 2012). Such disequilibrium is not evident in the exsolved Kaapvaal garnets but the sinusoidal and normal REE patterns of some of these garnets may be testimony to a refertilisation event well before the time of entrainment.

Akin to the model proposed above for the Kaapvaal samples, Chin *et al.* (2012) suggested that the protoliths of the Sierra Nevada garnet-bearing peridotites were spinel peridotites, formed by shallow melt depletion (1-2 GPa, 1300-1400 °C) followed by compression and cooling in the garnet stability field, as a consequence of progressive thickening of the Sierran arc lithosphere. Chin *et al.* (2015) modelled Al-diffusion profiles in the orthopyroxenes and combined these with Lu-Hf and Sm-Nd model ages to show that the

Sierran lithosphere cooled very quickly (<10 Myr) from 1250 to 750 °C, just after the peak of arc magmatism. One possible scenario is that the isochemical sub-solidus exsolution of garnet from orthopyroxene in sub-cratonic mantle occurred during cratonization and rapid lithospheric thickening at ~ 2.5 Ga. A detailed Sm-Nd and Lu-Hf isotopic investigation is now required to date closure temperatures for the exsolved clinopyroxene and garnet (see Shu et al., 2014). These timescales of exsolution could potentially distinguish between the different processes that have been proposed for the formation of cratonic lithosphere, *i.e.* evidence of rapid cooling would be consistent with models that invoke tectonic thickening whereas conductive cooling of a thermal boundary layer would require longer timescales.

Conclusions

(i) Orthopyroxenes (enstatite) found as megacrysts and also in mantle xenoliths entrained in kimberlites from southern parts of the Kaapvaal craton show evidence for isochemical exsolution of pyrope garnet and in some cases Cr-diopside. Spectacular microstructures formed by exsolved garnet vary from fine to coarse lamellae and are best preserved in orthopyroxene megacrysts. The diffusion length scale of garnet forming coarse lamellae in large (20 mm) orthopyroxene megacrysts is 2 mm. For smaller orthopyroxene grains (< 10 mm), found in peridotite xenoliths, diffusion lengths of Ca²⁺, Al³⁺ and Si⁴⁺ are such that garnet nucleates on orthopyroxene grain boundaries. These are most readily identified when they form interconnected networks or 'necklace' textures. They may also form discrete grains but establishing the origin of these is more enigmatic.

(ii) Pressure and temperature estimates reveal the orthopyroxenes with exsolved garnet were entrained from a wide depth interval (85-175 km) that occupies almost the whole of the garnet stability field in the Kaapvaal lithospheric mantle (Figure 12).

(iii) The recalculated compositions of many of the precursor (pre-exsolution) orthopyroxenes are characterised by high Mg#, Al₂O₃ and CaO contents. They resemble residues formed by adiabatic decompression melting in the shallow (spinel-facies) mantle but a reaction involving transformation from olivine by reaction with silica-rich fluids cannot be excluded. The temperatures of initial orthopyroxene formation are significantly higher -- and their pressures much less -- than those of their final equilibration, and it is proposed that garnet exsolution most likely occurred during lithospheric thickening. This may have been during cratonization (i.e. prior to 2.5 Ga) but further work is required to establish the timing of this. Analogous microstructures of garnet exsolution from orthopyroxene are persevered in peridotite mantle xenoliths from the Late Mesozoic Sierra Nevada continental arc. Here, where the tectonic setting is much better understood, and coexisting phases are not yet fully equilibrated, exsolution of garnet from orthopyroxene has been estimated to occur in ~ 10 Myr, i.e. very rapid (Chin et al., 2015).

(iv) Garnets exsolved from orthopyroxenes entrained from the lower parts of the sub-cratonic lithosphere appear to have undergone refertilisation by metasomatic melts and fluids but those entrained from much shallower depths (~90 km) are strongly-depleted in light rare earth elements and preserve their original isochemical exsolution compositions. This is a significant feature of the dataset because these compositions represent the closest approximation to those proposed for hypothetical pre-metasomatic garnets of any published to date. They provide important end member compositions in models of enrichment of highly-depleted peridotite in the lithospheric mantle by reactive percolation of fluids and melts, which in some cases involved the synchronous growth of diamond.

(v) The modal abundance of garnet formed by isochemical exsolution from orthopyroxene in the Kaapvaal sub-cratonic mantle and elsewhere is unclear but may prove

to be an important consideration in models put forward to explain the widespread occurrence and nature of garnet, and processes involved in the formation and stabilisation of Earth's most ancient continental lithospheric mantle.

Acknowledgements

The research presented in this manuscript formed the basis of the 45th Hallimond Lecture at the 50th annual meeting of the *Volcanic and Magmatic Studies Group* (University of Edinburgh, UK). I am sincerely grateful to the *Mineralogical Society* for this award. Research on garnet exsolution was inspired by the late J. Barry Dawson, who was a pioneer in the study of mantle xenoliths and continental magmatism. His extensive field work in Africa, systematic sample collection and incisive interpretations generated a wealth of publications that have greatly aided our understanding of Earth's mantle.

I thank Tim Holland and Michael Carpenter for their inspirational discussions on garnet exsolution. Electron microprobe analyses of orthopyroxene megacrysts were carried out by Alex Clarke as part of an MSci project at the University of Cambridge. Technical assistance with analyses of mineral chemistry was provided by Iris Buisman (electron microprobe, QEMSCAN®) and Jason Day (LA-ICP-MS) and I thank them warmly for their sustained support. The clarity of the manuscript was improved by the constructive comments of Yannick Bussweiler and an anonymous reviewer.

References

Aoki, K.-I., Fujimaki, H. & Kitamura, M. (1980). Exsolved garnet-bearing pyroxene megacrysts from some South African kimberlites. *Lithos* **13**, 269–279.

- Arndt, N. T., Coltice, N., Helmstaedt, H. & Gregoire, M. (2009). Origin of Archean subcontinental lithospheric mantle: Some petrological constraints. *Lithos* **109**, 61–71.
- Artemieva, I. M. (2011). *The Lithosphere*. Cambridge University Press.
- Aulbach, S. (2012). Craton nucleation and formation of thick lithospheric roots. *Lithos* **149**, 16–30.
- Bedini, R.-M., Blichert-Toft, J., Boyet, M. & Albarède, F. (2004). Isotopic constraints on the cooling of the continental lithosphere. *Earth and Planetary Science Letters* **223**, 99–111.
- Beeson, M. H. & Jackson, E. D. (1970). Origin of garnet pyroxenite xenoliths at Salt Lake crater. *Mineralogical Society of America Special Publication S 3*, 95–112.
- Begg, G. C. *et al.* (2009). The lithospheric architecture of Africa: Seismic tomography, mantle petrology, and tectonic evolution. *Geosphere* **5**, 23–50.
- Bell, D. R., Schmitz, M. D. & Janney, P. E. (2003). Mesozoic thermal evolution of the southern African mantle lithosphere. *Lithos* **71**, 273–287.
- Boyd, F. R. (1989). Compositional distinction between oceanic and cratonic lithosphere. *Earth and Planetary Science Letters* **96**, 15–26.
- Boyd, F. R. & Mertzman, S. A. (1987). Composition and structure of the Kaapvaal lithosphere, South Africa. **1**, 13–24.
- Boyd, F. R., Pearson, D. G., Nixon, P. H. & Mertzman, S. A. (1993). Low-calcium garnet harzburgites from southern Africa: their relations to craton structure and diamond crystallization. *Contributions to Mineralogy and Petrology* **113**, 352–366.
- Brey, G. P. & Kohler, T. (1990). Geothermobarometry in four-phase lherzolites II. New thermobarometers, and practical assessment of existing thermobarometers. *Journal of Petrology* **31**, 1353–1378.
- Brey, G. P., Kohler, T. & Nickel, K. G. (1990). Geothermobarometry in four-phase lherzolites I. Experimental results from 10 to 60 kb. *Journal of Petrology* **31**, 1313–1352.
- Burgess, S. R. & Harte, B. (1999). Tracing lithosphere evolution through the analysis of heterogeneous G9/G10 garnets in peridotite xenoliths, I: major element chemistry. *Proceedings of the 7th International Kimberlite Conference* 66–80.
- Burgess, S. R. & Harte, B. (2004). Tracing lithosphere evolution through the analysis of heterogeneous G9–G10 garnets in peridotite xenoliths, II: REE chemistry. *Journal of Petrology* **45**, 609–633.
- Bussweiler, Y., Stone, R. S., Pearson, D. G., Luth, R. W., Stachel, T., Kjarsgaard, B. A. & Menzies, A. (2016). The evolution of calcite-bearing kimberlites by melt-rock reaction: evidence from polymineralic inclusions within clinopyroxene and garnet megacrysts from Lac de Gras kimberlites, Canada. *Contributions to Mineralogy and Petrology* **171**, 65.

- Canil, D. (1991). Experimental evidence for the exsolution of cratonic peridotite from high-temperature harzburgite. *Earth and Planetary Science Letters* **106**, 64–72.
- Carlson, R. W., Pearson, D. G. & James, D. E. (2005). Physical, chemical, and chronological characteristics of continental mantle. *Reviews of Geophysics* **43**, doi:10.1029/2004RG000156.
- Chin, E. J., Lee, C.-T. A. & Blichert-Toft, J. (2015). Growth of upper plate lithosphere controls tempo of arc magmatism: Constraints from Al-diffusion kinetics and coupled Lu-Hf and Sm-Nd chronology. *Geochemical Perspectives Letters* **1**, 20–32.
- Chin, E. J., Lee, C.-T. A., Luffi, P. & Tice, M. (2012). Deep lithospheric thickening and refertilization beneath continental arcs: Case Study of the P, T and compositional evolution of peridotite xenoliths from the Sierra Nevada, California. *Journal of Petrology* **53**, 477–511.
- Cox, K. G., Smith, M. R. & Beswetherick, S. (1987). Textural studies of garnet lherzolites: evidence of exsolution from high-temperature harzburgites. *P.H. Nixon (Ed.), Mantle Xenoliths, John Wiley & Sons, Chichester, New York*. Chichester: Wiley, 537–550.
- Dawson, J. B. (1981). The nature of the upper mantle. *Mineralogical Magazine* **44**, 1–18.
- Dawson, J. B. (1987). Metasomatised harzburgites in kimberlite and alkaline magmas: enriched restites and “flushed” lherzolites. *In: Menzies, M.A. & Hawkesworth, C.J. (eds) Mantle metasomatism, Academic Press, London* 125–144.
- Dawson, J. B. (2004). A fertile harzburgite-garnet lherzolite transition: possible inferences for the roles of strain and metasomatism in upper mantle peridotites. *Lithos* **77**, 553–569.
- Dawson, J. B., Smith, J. V. & Hervig, R. L. (1980). Heterogeneity in upper-mantle lherzolites and harzburgites. *Philosophical Transactions of the Royal Society of London. Series A, Mathematical and Physical Sciences* **297**, 323–332.
- Dawson, P. J. B. (1980). The Megacryst Suite. *Kimberlites and Their Xenoliths*. Springer Berlin Heidelberg, 190–199.
- Doucet, L. S., Ionov, D. A., Golovin, A. V. & Pokhilenko, N. P. (2012). Depth, degrees and tectonic settings of mantle melting during craton formation: inferences from major and trace element compositions of spinel harzburgite xenoliths from the Udachnaya kimberlite, central Siberia. *Earth and Planetary Science Letters* **359–360**, 206–218.
- Eggler, D. H., McCallum, M. E. H. & Smith, C. B. (1979). Megacryst assemblages in kimberlite from Northern Colorado and Southern Wyoming: Petrology, geothermometry-barometry, and areal distribution. *In: Boyd, F. R. & Meyer, H. O. A. (eds) The Mantle Sample: Inclusion in Kimberlites and Other Volcanics*. American Geophysical Union, 213–226.
- Eggler, D. H. & Wendlandt, R. F. (1982). Experimental studies on the relationship between kimberlite magmas and partial melting of peridotite. *In: Meyer, H. O. A. & Boyd, F. R.*

- (eds) *Kimberlites, Diatremes, and Diamonds: Their Geology, Petrology, and Geochemistry*. American Geophysical Union, 330–338.
- Faryad, S. W., Dolejš, D. & Machek, M. (2009). Garnet exsolution in pyroxene from clinopyroxenites in the Moldanubian zone: constraining the early pre-convergence history of ultramafic rocks in the Variscan orogen. *Journal of Metamorphic Geology* **27**, 655–671.
- Gibson, S. A., Malarkey, J. & Day, J. A. (2008). Melt depletion and enrichment beneath the Western Kaapvaal Craton: Evidence from Finsch peridotite xenoliths. *Journal of Petrology* **49**, 1817–1852.
- Gibson, S. A., McMahon, S. C., Day, J. A. & Dawson, J. B. (2013). Highly-refractory lithospheric mantle beneath the Tanzanian Craton: evidence from Lashaine pre-metasomatic garnet-bearing peridotites. *Journal of Petrology* **54**, 1503–1546.
- Griffin, W. L., Fisher, N. I., Friedman, J., Ryan, C. G. & O'Reilly, S. Y. (1999a). Cr-pyrope garnets in the lithospheric mantle. I. Compositional systematics and relations to tectonic setting. *Journal of Petrology* **40**, 679–704.
- Griffin, W. L., O'Reilly, S. Y., Natapov, L. M. & Ryan, C. G. (2003). The evolution of lithospheric mantle beneath the Kalahari Craton and its margins. *Lithos* **71**, 215–241.
- Griffin, W., O'Reilly, S. & Ryan, C. (1999b). The composition and origin of sub-continental lithospheric mantle. *Mantle petrology: field observations and high-pressure experimentation: a tribute to Francis R. (Joe) Boyd*. The Geochemical Society Houston, 13–45.
- Grütter, H. S., Apter, D. B. & Kong, J. (1999). Crust-mantle coupling: evidence from mantle-derived xenocrystic garnets. Gurney, J. J., Gurney, J. L., Pascoe, M. D. & Richardson, S. H. (eds) *Proceedings Volume of 7th International Kimberlite Conference, Cape Town*. Cape Town: Red Roof Designs, 307–313.
- Grütter, H. S., Gurney, J. J., Menzies, A. H. & Winter, F. (2004). An updated classification scheme for mantle-derived garnet, for use by diamond explorers. *Lithos* **77**, 841–857.
- Grütter, H. S. & Tuer, J. (2009). Constraints on deep mantle tenor of Sarfartoq-area kimberlites (Greenland), based on modern thermobarometry of mantle-derived xenocrysts. *Lithos* **112**, Supplement 1, 124–129.
- Gurney, J. J., Jakob, W. R. O. & Dawson, J. B. (1979). Megacrysts from the Monastery Kimberlite Pipe, South Africa. In: Boyd, F. R. & Meyer, H. O. A. (eds) *The Mantle Sample: Inclusion in Kimberlites and Other Volcanics*. American Geophysical Union, 227–243.
- Gurney, J. J. & Switzer, G. S. (1973). The discovery of garnets closely related to diamonds in the Finsch pipe, South Africa. *Contributions to Mineralogy and Petrology* **39**, 103–116.

- Harte, B. (1983). Mantle peridotites and processes - the kimberlite sample. *Continental Basalts and Mantle Xenoliths* 46–91.
- Harte, B. & Gurney, J. J. (1975). Evolution of clinopyroxene and garnet in an eclogite nodule from the Roberts Victor kimberlite pipe, South Africa. *Physics and Chemistry of the Earth* **9**, 367–387.
- Harte, B. & Gurney, J. J. (1981). The mode of formation of chromium-poor megacryst suites from kimberlites. *The Journal of Geology* **89**, 749–753.
- Harte, B., Hunter, R. H. & Kinny, P. D. (1993). Melt geometry, movement and crystallization, in relation to mantle dykes, veins and metasomatism. *Philosophical Transactions of the Royal Society of London A: Mathematical, Physical and Engineering Sciences* **342**, 1–21.
- Herzberg, C. (1993). Lithosphere peridotites of the Kaapvaal craton. *Earth and Planetary Science Letters* **120**, 13–29.
- Herzberg, C. (2004). Geodynamic information in peridotite petrology. *Journal of Petrology* **45**, 2507–2530.
- Herzberg, C. & Rudnick, R. (2012). Formation of cratonic lithosphere: An integrated thermal and petrological model. *Lithos* **149**, 4–15.
- Hirschmann, M. M. (2000). Mantle solidus: Experimental constraints and the effects of peridotite composition. *Geochemistry Geophysics Geosystems* **1**, 26 PP.
- Ivanic, T. J., Harte, B. & Gurney, J. J. (2016). A discussion of “Mineralogical controls on garnet composition in the cratonic mantle” by Hill et al., *Contributions to Mineralogy and Petrology* (2015) 169:13. *Contributions to Mineralogy and Petrology* **171**, 1–4.
- Jerde, E. A., Taylor, L. A., Crozaz, G. & Sobolev, N. V. (1993). Exsolution of garnet within clinopyroxene of mantle eclogites: major- and trace-element chemistry. *Contributions to Mineralogy and Petrology* **114**, 148–159.
- Johnson, K. T. M. (1998). Experimental determination of partition coefficients for rare earth and high-field-strength elements between clinopyroxene, garnet, and basaltic melt at high pressures. *Contributions to Mineralogy and Petrology* **133**, 60–68.
- Jordan, T. H. (1979). Mineralogies, densities and seismic velocities of garnet lherzolites and their geophysical implications. In F.R. Boyd & H.O. Meyer, (Eds.) *The Mantle Sample: Inclusions in Kimberlites and Other Volcanics, Proceedings of the 2nd International Kimberlite Conference, AGU, Washington D.C.* 1–14.
- Kelemen, P. B., Hart, S. . & Bernstein, S. (1998). Silica enrichment in the continental upper mantle via melt/rock reaction. *Earth and Planetary Science Letters* **164**, 387–406.
- Kennedy, C. S. & Kennedy, G. C. (1976). The equilibrium boundary between graphite and diamond. *Journal of Geophysical Research* **81**, 2467–2470.
- Kesson, S. E. & Ringwood, A. E. (1989). Slab-mantle interactions: 2. The formation of diamonds. *Chemical Geology* **78**, 97–118.

- Klemme, S., O'Neill, H.S.C., 2000. The near-solidus transition from garnet lherzolite to spinel lherzolite. *Contributions to Mineralogy and Petrology* **138**, 237–248.
- Kramers, J. D., Roddick, J. C. M. & Dawson, J. B. (1983). Trace element and isotope studies on veined, metasomatic and “MARID” xenoliths from Bultfontein, South Africa. *Earth and Planetary Science Letters* **65**, 90–106.
- Lazarov, M., Brey, G. P. & Weyer, S. (2012). Evolution of the South African mantle—a case study of garnet peridotites from the Finsch diamond mine (Kaarvaal craton); Part 2: Multiple depletion and re-enrichment processes. *Lithos* **154**, 210–223.
- Lazarov, M., Woodland, A. B. & Brey, G. P. (2009). Thermal state and redox conditions of the Kaarvaal mantle: A study of xenoliths from the Finsch mine, South Africa. *Lithos* **112**, Supplement 2, 913–923.
- Lee, C.-T. A. & Chin, E. J. (2014). Calculating melting temperatures and pressures of peridotite protoliths: Implications for the origin of cratonic mantle. *Earth and Planetary Science Letters* **403**, 273–286.
- Lee, C.-T., Luffi, P. & Chin, E. J. (2011). Building and destroying continental mantle. *Annual Review of Earth and Planetary Sciences* **39**, 59–90.
- Mather, K. A., Pearson, D. G., McKenzie, D., Kjarsgaard, B. A. & Priestley, K. (2011). Constraints on the depth and thermal history of cratonic lithosphere from peridotite xenoliths, xenocrysts and seismology. *Lithos* **125**, 729–742.
- McDonough, W. & Sun, S. -s. (1995). The composition of the Earth. *Chemical Geology* **120**, 223–253.
- McKenzie, D., Jackson, J. & Priestley, K. (2005). Thermal structure of oceanic and continental lithosphere. *Earth and Planetary Science Letters* **233**, 337–349.
- Menzies, M. & Murphy V. R. (1980). Enriched mantle: Nd and Sr isotopes in diopsides from kimberlite nodules. *Nature* **283**, 634–636.
- Michaut, C. & Jaupart, C. (2007). Secular cooling and thermal structure of continental lithosphere. *Earth and Planetary Science Letters* **257**, 83–96.
- Moore, A. & Costin, G. (2016). Kimberlitic olivines derived from the Cr-poor and Cr-rich megacryst suites. *Lithos* **258–259**, 215–227.
- Nair, S. K., Gao, S. S., Liu, K. H. & Silver, P. G. (2006). Southern African crustal evolution and composition: Constraints from receiver function studies. *Journal of Geophysical Research: Solid Earth* **111**, B02304.
- Nickel, K. G. & Green, D. H. (1985). Empirical geothermobarometry for garnet peridotites and implications for the nature of the lithosphere, kimberlites and diamonds. *Earth and Planetary Science Letters* **73**, 158–170.
- Nimis, P. & Grütter, H. (2009). Internally consistent geothermometers for garnet peridotites and pyroxenites. *Contributions to Mineralogy and Petrology* **159**, 411–427.

- O'Hara, M. J., Saunders, M. J. & Mercy, E. L. P. (1975). Garnet-peridotite, primary ultrabasic magma and eclogite; Interpretation of upper mantle processes in kimberlite. *Physics and Chemistry of the Earth* **9**, 571–604.
- Orman, J. A. V., Grove, T. L., Shimizu, N. & Layne, G. D. (2002). Rare earth element diffusion in a natural pyrope single crystal at 2.8 GPa. *Contributions to Mineralogy and Petrology* **142**, 416–424.
- Pearson, D. G., Brenker, F. E., Nestola, F., McNeill, J., Nasdala, L., Hutchison, M. T., Matveev, S., Mather, K., Silversmit, G., Schmitz, S., Vekemans, B., & Vincze L. (2014). Hydrous mantle transition zone indicated by ringwoodite included within diamond. *Nature* **507**, 221–224.
- Pearson, D. G., Carlson, R. W., Shirey, S. B., Boyd, F. R. & Nixon, P. H. (1995). Stabilisation of Archaean lithospheric mantle: A Re-Os isotope study of peridotite xenoliths from the Kaapvaal craton. *Earth and Planetary Science Letters* **134**, 341–357.
- Pearson, D. G. & Wittig, N. (2008). Formation of Archaean continental lithosphere and its diamonds: the root of the problem. *Journal of the Geological Society* **165**, 895–914.
- Pearson, D. G. & Wittig, N. (2013). The formation and evolution of cratonic mantle lithosphere - Evidence from mantle xenoliths. *Treatise in Geochemistry*. Elsevier.
- Peslier, A. H., Woodland, A. B., Bell, D. R. & Lazarov, M. (2010). Olivine water contents in the continental lithosphere and the longevity of cratons. *Nature* **467**, 78–81.
- Priestley, K. & McKenzie, D. (2013). The relationship between shear wave velocity, temperature, attenuation and viscosity in the shallow part of the mantle. *Earth Planet. Sci. Letts.* **381**, 78–91.
- Richter, F. M. (1988). A major change in the thermal state of the Earth at the Archean-Proterozoic boundary: Consequences for the nature and preservation of continental lithosphere. *Journal of Petrology Special Lithosphere Issue*, 39–52.
- Roach, I. C. (2004). Mineralogy, textures and P–T relationships of a suite of xenoliths from the Monaro Volcanic Province, New South Wales, Australia. *Journal of Petrology* **45**, 739–758.
- Rudnick, R. L., McDonough, W. F. & Orpin, A. (1994). Northern Tanzania peridotite xenoliths: a comparison with Kaapvaal xenoliths and inferences of metasomatic reactions. Meyer, H.O.A. & Leonardos, O.H. (eds). *Kimberlites, Related Rocks and Mantle Xenoliths. Proceedings 5th International Kimberlite Conf* 336–353.
- Russell, J. K., Porritt, L. A., Lavallée, Y. & Dingwell, D. B. (2012). Kimberlite ascent by assimilation-fuelled buoyancy. *Nature* **481**, 352–356.
- Saltzer, R. L., Chatterjee, N. & Grove, T. L. (2001). The spatial distribution of garnets and pyroxenes in mantle peridotites: Pressure–temperature history of peridotites from the Kaapvaal craton. *Journal of Petrology* **42**, 2215–2229.

- Sautter, V. & Harte, B. (1988). Diffusion gradients in an eclogite xenolith from the Roberts Victor Kimberlite Pipe: 1. Mechanism and evolution of garnet exsolution in Al₂O₃-rich clinopyroxene. *Journal of Petrology* **29**, 1325–1352.
- Sautter, V. & Harte, B. (1990). Diffusion gradients in an eclogite xenolith from the Roberts Victor kimberlite pipe: (2) kinetics and implications for petrogenesis. *Contributions to Mineralogy and Petrology* **105**, 637–649.
- Schulze, D. J. (1995). Low-Ca garnet harzburgites from Kimberley, South Africa: Abundance and bearing on the structure and evolution of the lithosphere. *Journal of Geophysical Research: Solid Earth* **100**, 12513–12526.
- Schutt, D. L. & Leshner, C. E. (2010). Compositional trends among Kaapvaal Craton garnet peridotite xenoliths and their effects on seismic velocity and density. *Earth and Planetary Science Letters* **300**, 367–373.
- Shu, Q. & Brey, G. P. (2015). Ancient mantle metasomatism recorded in subcalcic garnet xenocrysts: Temporal links between mantle metasomatism, diamond growth and crustal tectonomagmatism. *Earth and Planetary Science Letters* **418**, 27–39.
- Shu, Q., Brey, G. P., Gerdes, A. & Hofer, H. E. (2013). Geochronological and geochemical constraints on the formation and evolution of the mantle underneath the Kaapvaal craton: Lu–Hf and Sm–Nd systematics of subcalcic garnets from highly depleted peridotites. *Geochimica et Cosmochimica Acta* **113**, 1–20.
- Shu, Q., Brey, G. P., Gerdes, A. & Hofer, H. E. (2014). Mantle eclogites and garnet pyroxenites—the meaning of two-point isochrons, Sm–Nd and Lu–Hf closure temperatures and the cooling of the subcratonic mantle. *Earth and Planetary Science Letters* **389**, 143–154.
- Simon, N. S. C., Carlson, R. W., Pearson, D. G. & Davies, G. R. (2007). The origin and evolution of the Kaapvaal cratonic lithospheric mantle. *Journal of Petrology* **48**, 589–625.
- Simon, N. S. C., Irvine, G. J., Davies, G. R., Pearson, D. G. & Carlson, R. W. (2003). The origin of garnet and clinopyroxene in “depleted” Kaapvaal peridotites. *Lithos* **71**, 289–322.
- Smith, C. B., Gurney, J. J., Skinner, E. M. W., Clement, C. R. & Ebrahim, N. (1985). Geochemical character of Southern African kimberlites; a new approach based on isotopic constraints. *South African Journal of Geology* **88**, 267–280.
- Sobolev, N. V., Lavrent'ev, Y. G., Pokhilenko, N. P. & Usova, L. V. (1973). Chrome-rich garnets from the kimberlites of Yakutia and their parageneses. *Contributions to Mineralogy and Petrology* **40**, 39–52.
- Soltys, A., Giuliani, A., Phillips, D., Kamenetsky, V. S., Maas, R., Woodhead, J. & Rodemann, T. (2016). In-situ assimilation of mantle minerals by kimberlitic magmas — Direct evidence from a garnet wehrlite xenolith entrained in the Bultfontein kimberlite (Kimberley, South Africa). *Lithos* **256–257**, 182–196.

- Stachel, T., Aulbach, S., Brey, G. P., Harris, J. W., Leost, I., Tappert, R. & Viljoen, K. S. (2004). The trace element composition of silicate inclusions in diamonds: a review. *Lithos* **77**, 1–19.
- Stachel, T., Brey, G. P. & Harris, J. W. (2000). Kankan diamonds (Guinea) I: from the lithosphere down to the transition zone. *Contributions to Mineralogy and Petrology* **140**, 1–15.
- Stachel, T., Brey, G. P. & Harris, J. W. (2005). Inclusions in sublithospheric diamonds: Glimpses of deep Earth. *Elements* **1**, 73–78.
- Stachel, T. & Harris, J. W. (1997). Diamond precipitation and mantle metasomatism - evidence from the trace element chemistry of silicate inclusions in diamonds from Akwatia, Ghana. *Contributions to Mineralogy and Petrology* **129**, 143–154.
- Stachel, T. & Harris, J. W. (2008). The origin of cratonic diamonds — Constraints from mineral inclusions. *Ore Geology Reviews* **34**, 5–32.
- Stachel, T., Viljoen, K. S., Brey, G. . & Harris, J. W. (1998). Metasomatic processes in Iherzolitic and harzburgitic domains of diamondiferous lithospheric mantle: REE in garnets from xenoliths and inclusions in diamonds. *Earth and Planetary Science Letters* **159**, 1–12.
- Stephens, W. E. & Dawson, J. B. (1977). Statistical comparison between pyroxenes from kimberlites and their associated xenoliths. *The Journal of Geology* **85**, 433–449.
- Taylor, L. A., Anand, M., Promprated, P., Floss, C. & Sobolev, N. V. (2003). The significance of mineral inclusions in large diamonds from Yakutia, Russia. *American Mineralogist* **88**, 912–920.
- Taylor, W. R. (1998). An experimental test of some geothermometer and geobarometer formulations for upper mantle peridotites with application to the thermobarometry of fertile Iherzolite and garnet websterite. *Neues Jahrbuch Fur Mineralogie Abhandlungen* **172**, 381– 408.
- Tuff, J. & Gibson, S. A. (2006). Trace-element partitioning between garnet, clinopyroxene and Fe-rich picritic melts at 3 to 7 GPa. *Contributions to Mineralogy and Petrology* **153**, 369–387.
- von Seckendorff, V. & O'Neill, H. S. C. (1993). An experimental study of Fe-Mg partitioning between olivine and orthopyroxene at 1173, 1273 and 1423 K and 1.6 GPa. *Contributions to Mineralogy and Petrology* **113**, 196–207.
- Walker, R. ., Carlson, R. ., Shirey, S. . & Boyd, F. . (1989). Os, Sr, Nd, and Pb isotope systematics of southern African peridotite xenoliths: Implications for the chemical evolution of subcontinental mantle. *Geochimica et Cosmochimica Acta* **53**, 1583–1595.
- Walter, M. J. (1998). Melting of garnet peridotite and the origin of komatiite and depleted lithosphere. *Journal of Petrology* **39**, 29–60.

Walter, M. J., Kohn, S. C., Araujo, D., Bulanova, G. P., Smith, C. B., Gaillou, E., Wang, J., Steele, A. & Shirey, S. B. (2011). Deep mantle cycling of oceanic crust: Evidence from diamonds and their mineral inclusions. *Science* **334**, 54–57.

Wilkinson, J. F. G. (1976). Some subcalcic clinopyroxenites from Salt Lake Crater, Oahu, and their petrogenetic significance. *Contributions to Mineralogy and Petrology* **58**, 181–201.

Ziberna, L., Nimis, P., Zanetti, A., Marzoli, A. & Sobolev, N. V. (2013). Metasomatic processes in the central Siberian cratonic mantle: Evidence from garnet xenocrysts from the Zagadochnaya kimberlite. *Journal of Petrology* egt051.

Figure captions

Figure 1. Change in density of mantle peridotite as garnet is removed during partial melting (after Artemieva, 2011)

Figure 2. CaO versus Cr₂O₃ classification plot for mantle garnets in equilibrium with orthopyroxene and/or clinopyroxene, after Sobolev et al. (1973) and Grütter et al. (2004). The compositions are shown for garnets exsolved in orthopyroxene megacrysts and orthopyroxenes found in mantle peridotites entrained by various kimberlite pipes from the Kaapvaal craton. Garnets in equilibrium with primitive mantle melts are characterised by ~2 wt. % Cr₂O₃ and 4 to 5 wt. % CaO. In garnet lherzolites, orthopyroxene and clinopyroxene buffer the effects of moderate degrees of melt depletion which causes the Ca and Cr contents of garnets increase until all of the clinopyroxene is exhausted (Grütter *et al.*, 1999: 199; Stachel and Harris, 2008). Data are from [Table 2](#). The field of discrete and exsolved garnets found in peridotites from the Sierra Nevada continental arc (Chin *et al.*, 2012) is shown for comparison (see text for discussion).

Figure 3. Hand specimen images of enstatite megacrysts with exsolved pyrope garnet and Cr-diopside.

Figure 4. Photomicrographs (in cross polarised light) illustrating the range of exsolution textures involving garnet and sometimes clinopyroxene in mantle-derived orthopyroxenes from the Kaapvaal craton. (a) Exsolution lamellae of clinopyroxene and blebs of garnet in an orthopyroxene megacryst (BD1959, Wesselton; P=39 kbar, T=940 °C); (b) Exsolution lamellae of garnet in an orthopyroxene megacryst (BD1951, Bultfontein, Kimberley; P=37 kbar, T= 904 °C); and (c) Necklace texture of garnet around orthopyroxene in a peridotite xenolith (BD2015/3a, Frank Smith Mine; P=35 kbar, T=940 °C).

Figure 5. Al₂O₃ versus CaO contents of mantle orthopyroxenes from different tectonic settings (modified from Gibson *et al.*, 2008). Exsolution of garnet and in some cases clinopyroxene decreases Al₂O₃ and CaO contents so that megacrysts that once had comparable compositions to those found in off-craton spinel lherzolites now resemble those found in on-craton garnet peridotites. Data are from [Table 2](#). Orthopyroxenes found in peridotites from the Sierra Nevada continental arc (Chin *et al.*, 2012) are shown for comparison (see text for discussion).

Figure 6. Chondrite-normalised rare-earth-element plots illustrating the range of compositions of garnets exsolved from orthopyroxene found in Kaapvaal mantle megacrysts and peridotites. The various rare-earth-element patterns displayed by garnets found in mantle peridotites from the Tanzanian craton (Gibson *et al.*, 2013) are shown for comparison as are the compositions of garnets in equilibrium with convecting mantle melts (Tuff and Gibson, 2006). Data are from [Table 3](#). Chondrite normalisation factors are from McDonough & Sun (1995)

Figure 7. (a) Composite image of orthopyroxene megacryst BD3736/1 (taken in cross polarised light) illustrating the various styles and length scales of exsolution. (b) QEMSCAN®

image of orthopyroxene megacryst BD3736/1. Note the different orientations of exsolved pyrope garnet and Cr-diopside. Distance between coarse garnet lamellae is 4 mm.

Figure 8. Photomicrograph showing the relationship between coarse exsolution lamellae of pyrope garnet and spindle-shaped blebs of exsolved Cr-diopside in orthopyroxene megacryst BD3736/1. See Figure 7 for location of image in relation to whole megacryst.

Figure 9. Comparison of equilibration temperatures estimated for orthopyroxene megacrysts using the two-pyroxene solvus thermometer of Taylor (1998) and the Ca-in-orthopyroxene thermometer of Brey & Kohler (1990). Dashed lines are 60 °C tolerance limits from a 1:1 correlation (thick solid line) of the thermometers as suggested by Nimis & Grütter (2009). *P-T* data are from [Table 2](#).

Figure 10. Temperature vs depth profile through the Kaapvaal craton. The conductive geotherm is calculated using the *P-T* estimates for Finsch peridotites (data from Gibson *et al.*, 2008; Lazarov *et al.*, 2009), a crustal thickness of 38 km (Nair *et al.*, 2006) and an ambient mantle potential temperature of 1315 °C in the program FITPLOT (McKenzie *et al.*, 2005). *P-T* estimates for Finsch peridotites are from the same geo-thermometers and -barometers as the orthopyroxene megacrysts, i.e. the formulations of Taylor (1998), Brey *et al.* (1990) and Nickel & Green (1985). *P-T* data are from [Table 2](#). ΔT is the difference in temperature of the anhydrous peridotite solidus (Hirschmann, 2000) and the conductive geotherm at a given pressure. The stability fields of graphite and diamond, and orthopyroxene and garnet, are from Kennedy & Kennedy (1976) and Canil (1991), respectively. The spinel-garnet transition is from Klemme & O'Neill (2000). See text for discussion of exsolution textures in BD3736/1.

Figure 11. Comparison of chondrite-normalised rare-earth element (REE) patterns for garnets: (a) exsolved in Kaapvaal orthopyroxene megacryst BD3636/1 with: (b) from Sierra Nevada peridotites (Chin *et al.*, 2012); (c) with ultra-depleted CaO contents found at Lashaine, Tanzania (Gibson *et al.*, 2013); (d) and (e) present in peridotitic diamond inclusions from Kankan, Yakutia and Roberts Victor Mine (Stachel *et al.*, 1998, 2000; Taylor *et al.*, 2003); and (f) with rare earth element patterns akin to those typical of Iherzolite and harzburgite paragenesis (Stachel and Harris, 2008). The former have flat middle-to-heavy REE patterns while the latter are distinguished by their sinusoidal patterns.

Figure 12. Schematic illustration of the lithospheric mantle beneath the Kaapvaal craton, highlighting the large depth interval (90 km) over which garnet has exsolved from orthopyroxene. The thickness of the lithosphere (mechanical boundary layer) beneath the Kaapvaal craton is taken from the conductive geotherm calculated for Finsch Mine (see Figure 10). The graphite-diamond stability field is from Kennedy & Kennedy (1976). Mantle metasomatism is pervasive in the lowermost (~75 km) of the lithosphere.

Figure 1

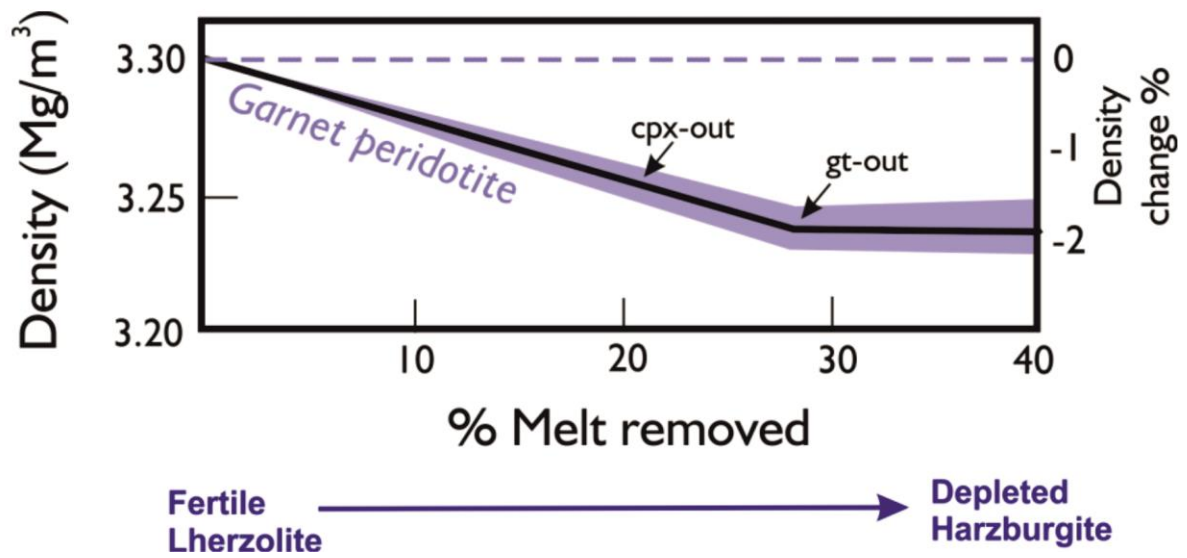


Figure 2

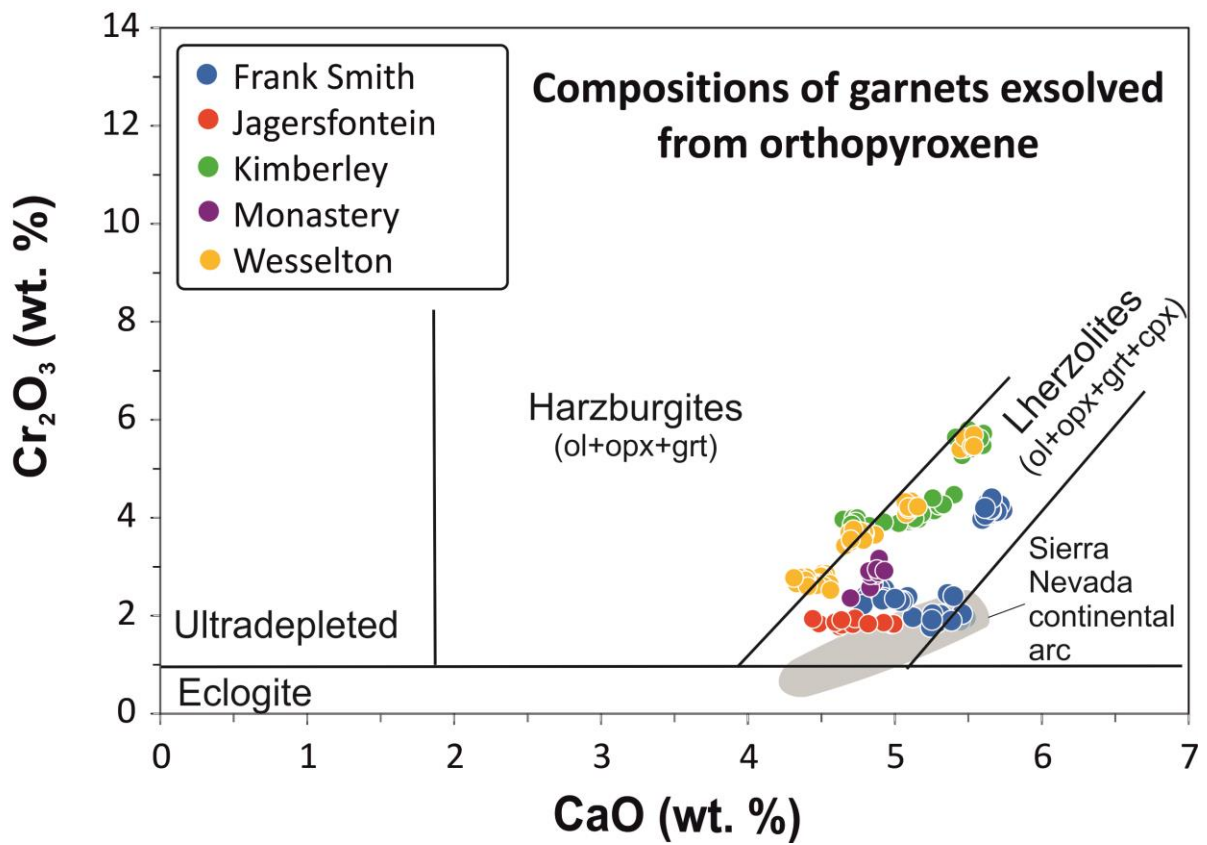


Figure 3

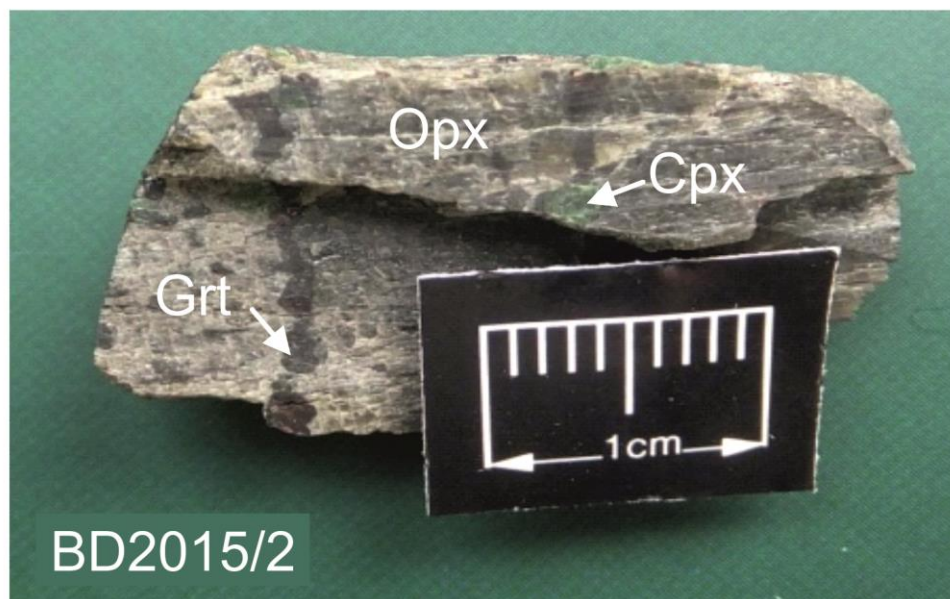
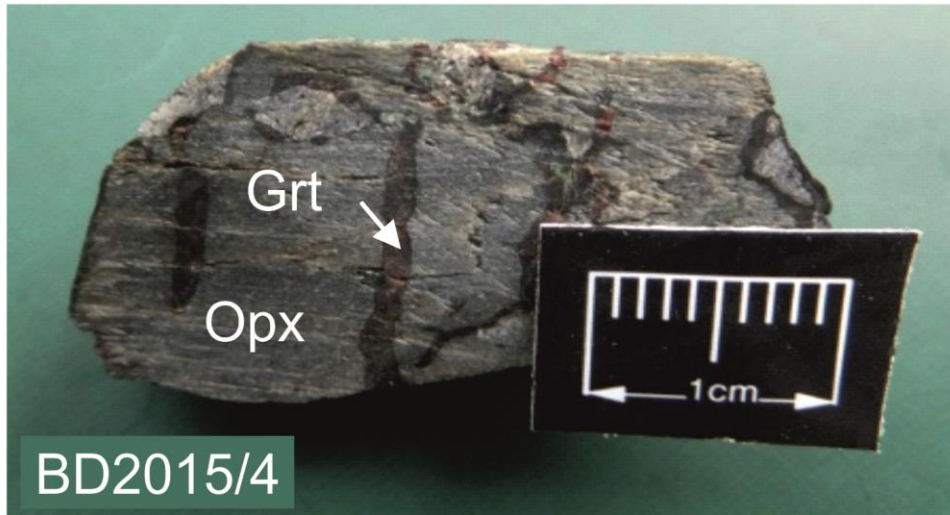
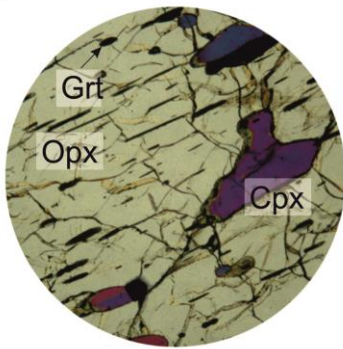
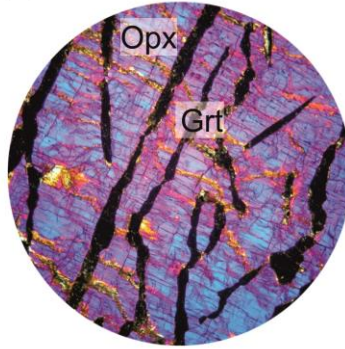


Figure 4

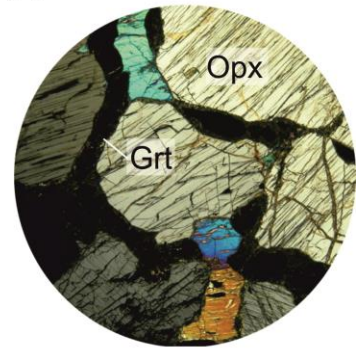
(a) BD1959



(b) BD1951



(c) BD2015/3a



2 mm

Figure 5

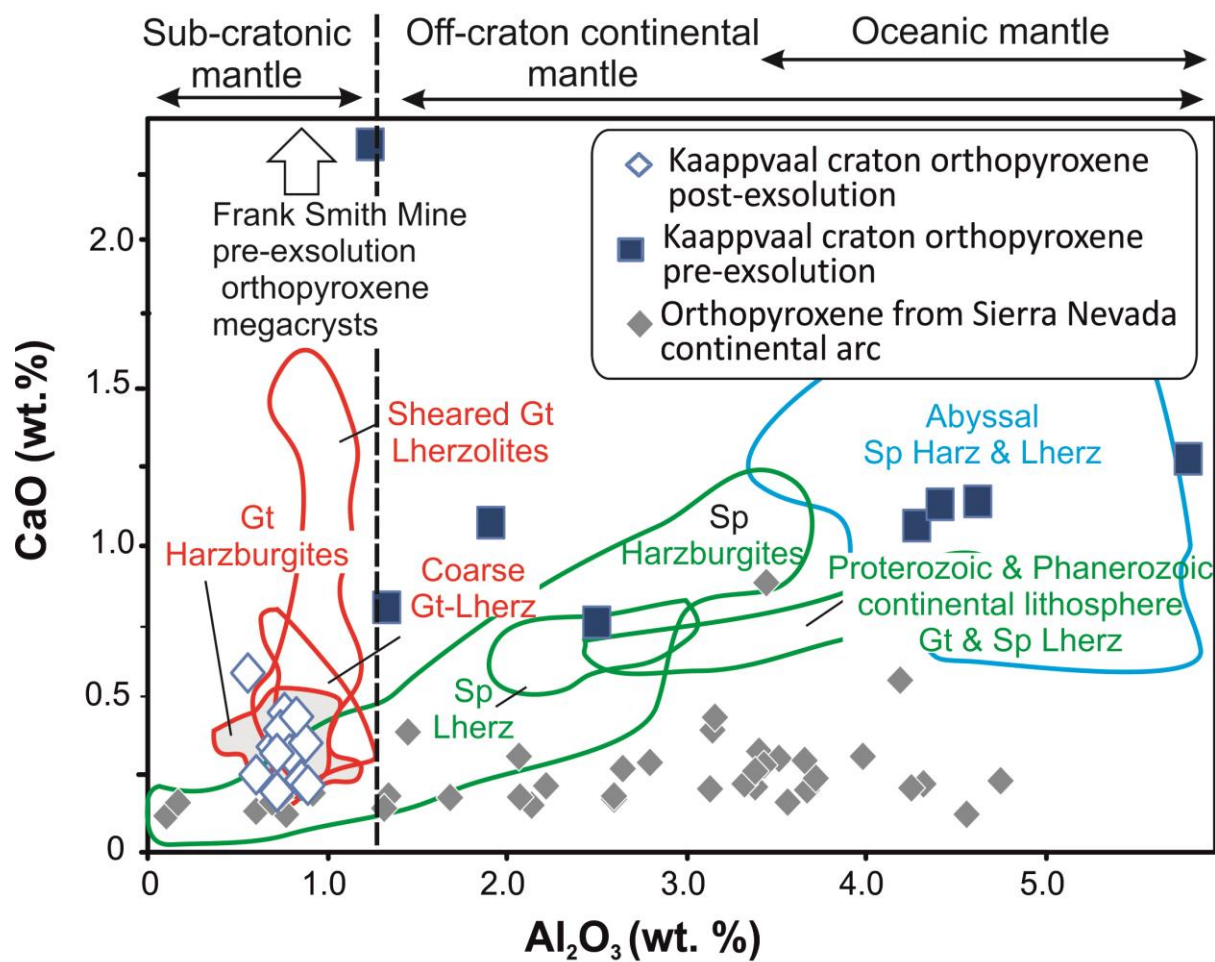


Figure 6

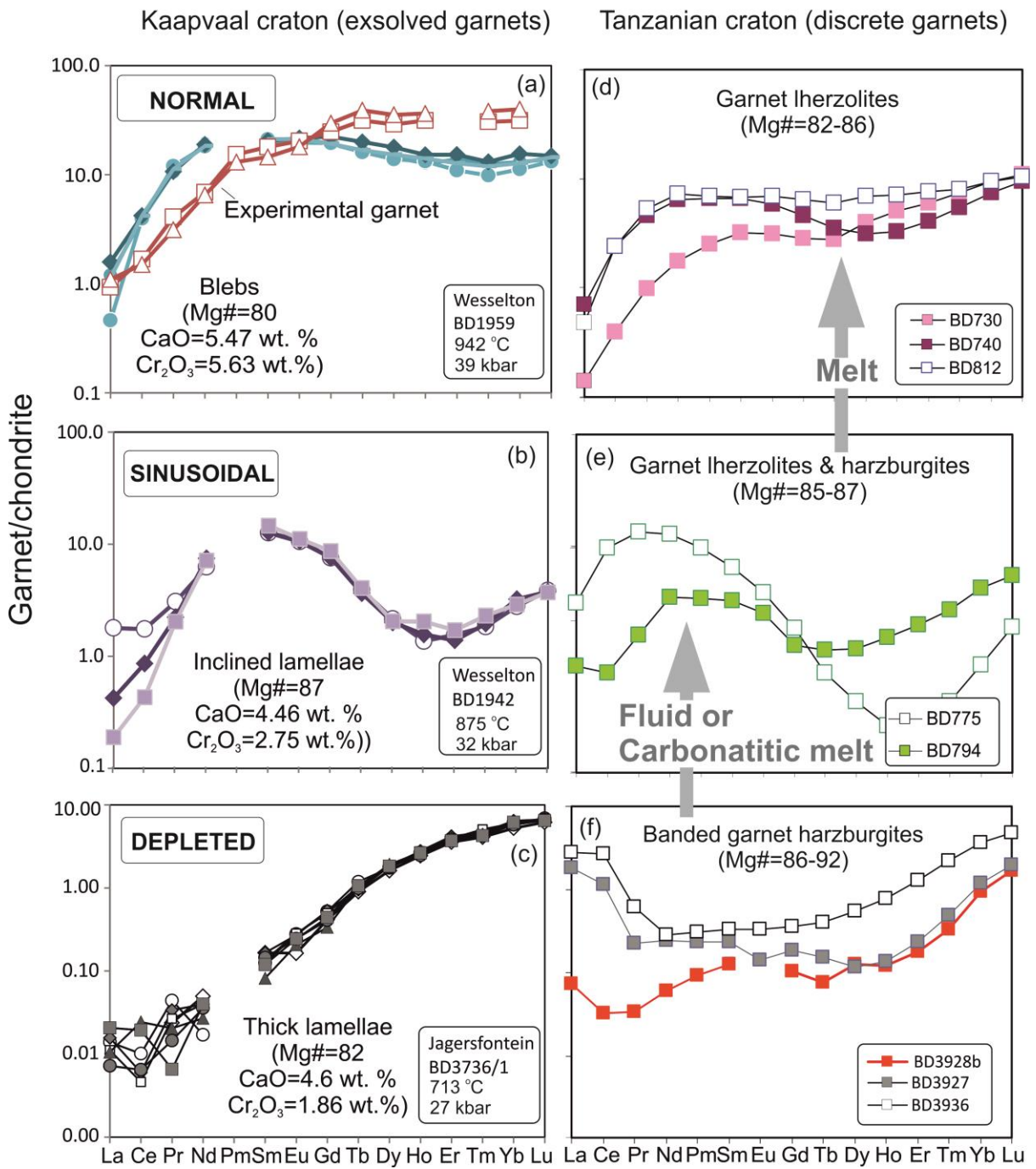


Figure 7

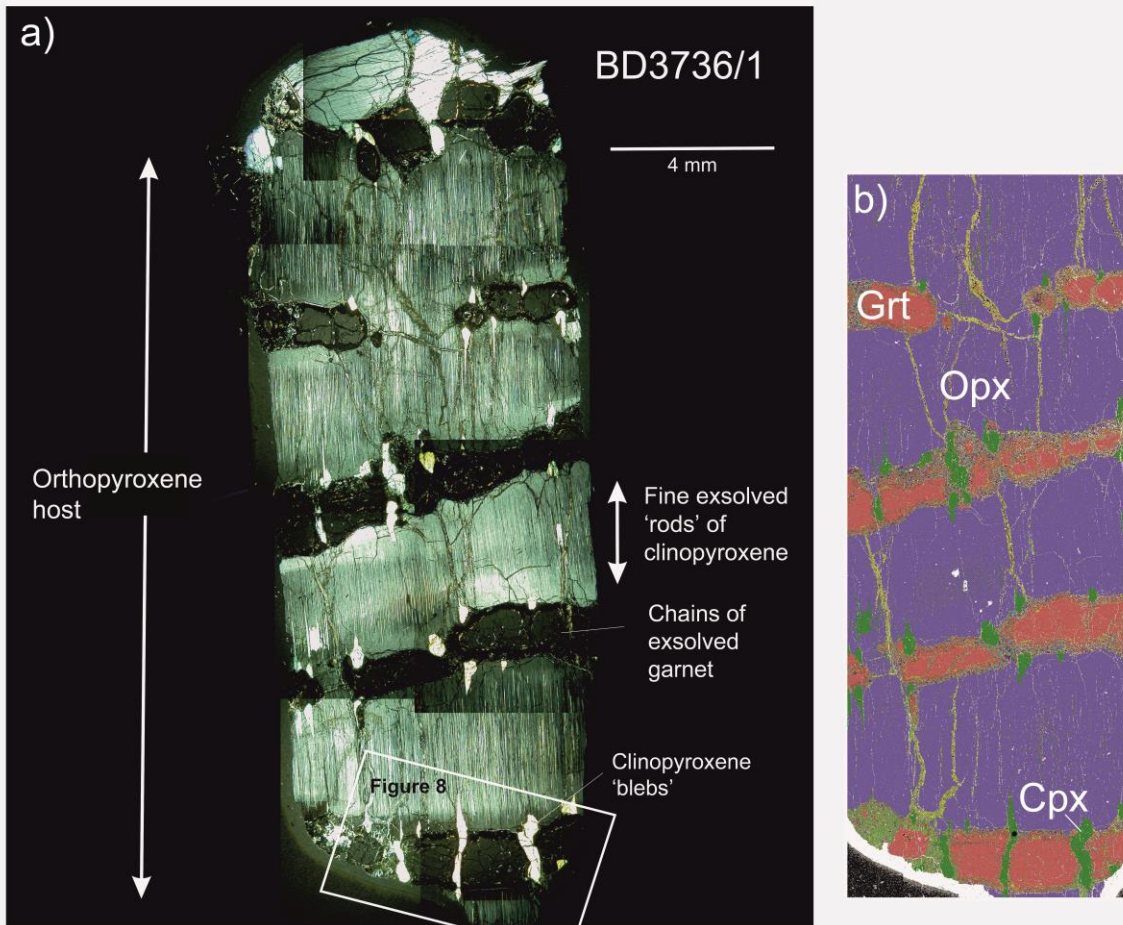


Figure 8

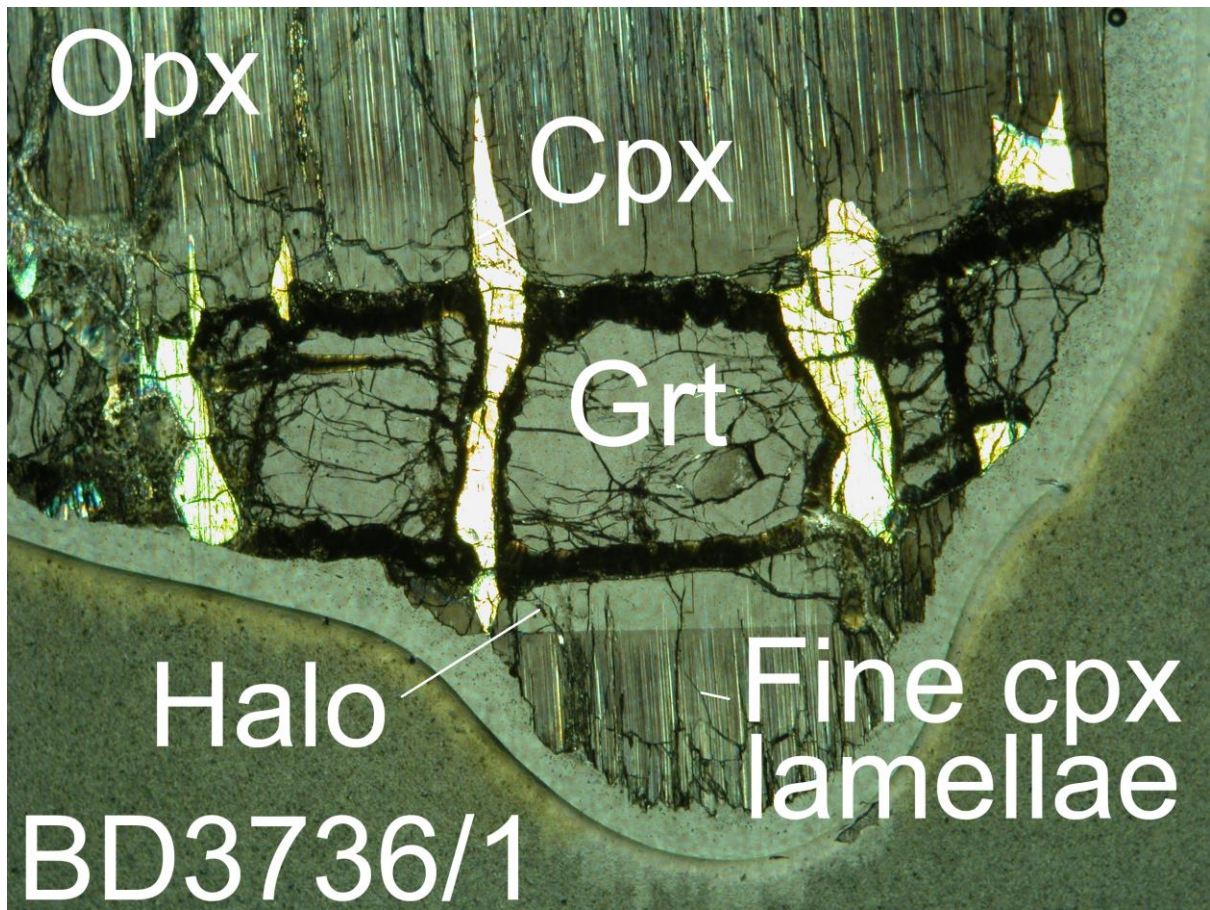


Figure 9

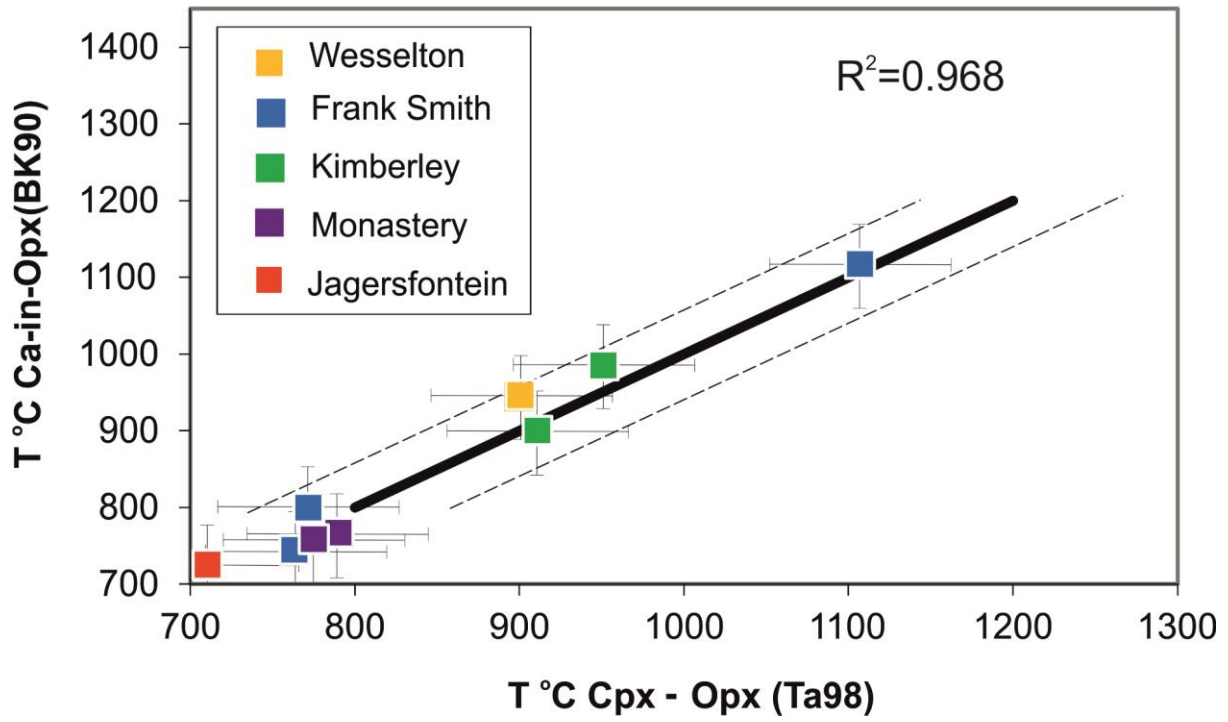


Figure 10

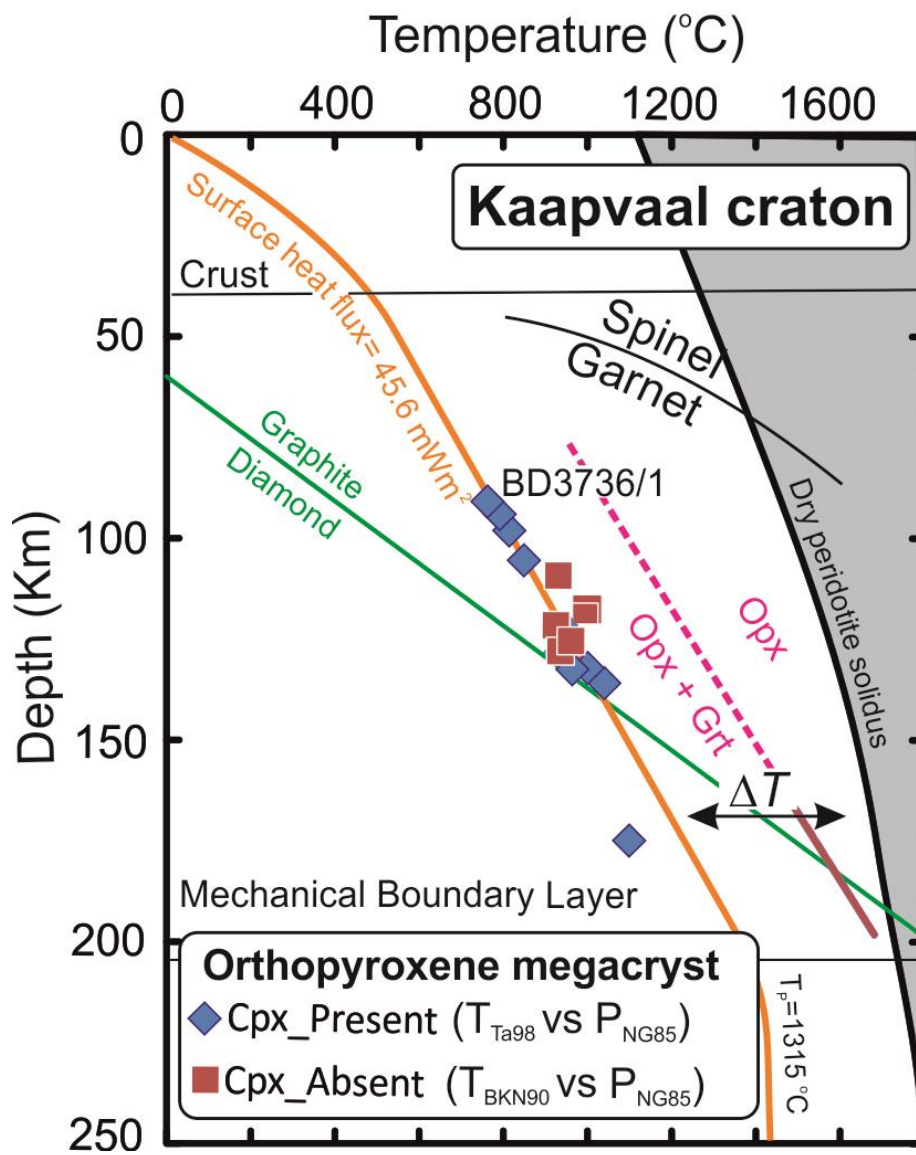


Figure 11

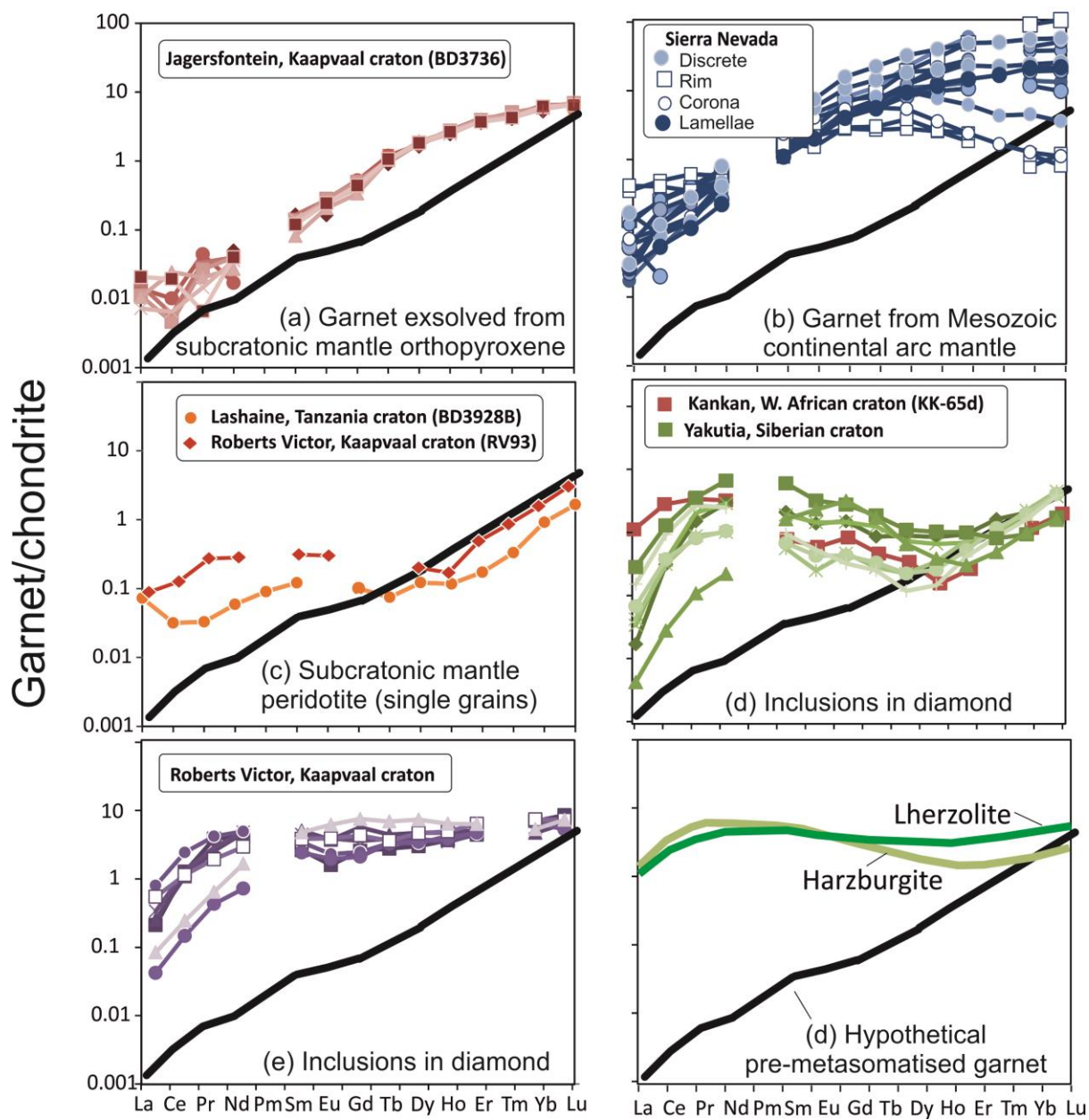


Figure 12

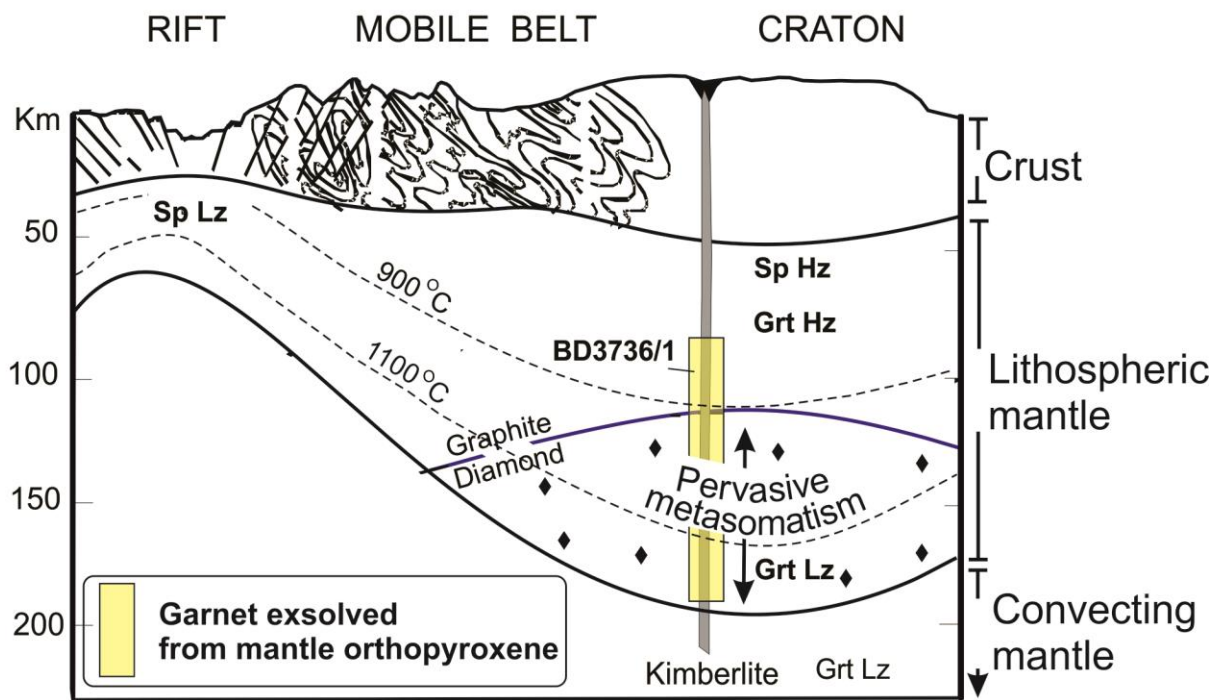


Table 5. Modal mineralogies for the Kaapvaal and Slave cratons

Craton	OI	Opx	Cpx	Gt	Bulk Mg#
Kaapvaal average	65	24	4	7	92.3
Kaapvaal average	65.5	26.9	6.1	1.3	92
Slave average	79	13	2	6	91.9
Archean average	79	13	2	6	93